AN INVESTIGATION OF DESCRIBING FUNCTION ERROR ESTIMATES

A Thesis

Presented to

the Faculty of Graduate Studies and Research

The University of Manitoba

In Partial Fulfillment

of the Requirements for the Degree

Master of Science

by

Glenn William Duncan

February 1967

ABSTRACT

by

Glenn William Duncan

AN INVESTIGATION OF DESCRIBING
FUNCTION ERROR ESTIMATES

The accuracy of the describing function method for the analysis of nonlinear feedback systems was investigated. Attention was restricted in general to autonomous systems and in particular to an article published in July 1965 by Garber and Rozenvasser. Several observations were made about the Garber - Rozenvasser technique and about an example given in the article. A "shift of gain" procedure was unsuccessful as a method of improving the Garber - Rozenvasser estimates. The usefulness of the estimates in cases for which the describing function method might fail was discussed. By analog simulation experimental results were obtained for several systems as a check on the estimates. The liberality of the estimated bounds on the maximum magnitude of the response prompted an experimental check of the Garber - Rozenvasser example system, with interesting results. The plotting of "A - w diagrams" was studied. A possible method of tightening Garber and Rozenvasser's bound on the effect of the higher harmonics in the response was outlined, but an example revealed that at best the method would yield a small improvement for a large amount of work.

ACKNOWLEDGMENTS

I wish to thank my thesis adviser, Professor R. A. Johnson of the Department of Electrical Engineering, the University of Manitoba, for his kind help and guidance throughout this investigation.

Thanks are also extended to the National Research Council of Canada for providing the financial support for my work, and to John P. Seddon for his suggestions concerning analog and digital computation.

TABLE OF CONTENTS

CHAPTER PAGE

LIST OF TABLES

LIST OF FIGURES

FIGURE PAGE

CHAPTER I

INTRODUCTION AND STATEMENT OF THE PROBLEM

I. THE DESCRIBING FUNCTION METHOD

Background information

The describing function method for the analysis of nonlinear feedback control systems was developed independently by workers in five different countries -- by Kochenburger in the United States, Goldfarb in the U.S.S.R., Oppelt in Germany, Tustin in England, and Dutilh in France.

For linear systems the principle of superposition holds, a sinusoidal excitation produces a sinusoidal response of different amplitude and phase, but of the same frequency, and stability is well defined in that the system is either stable or unstable regardless of the excitation and the initial conditions. As a result of these characteristics linear system theory has been thoroughly developed. In nonlinear systems, on the other hand, the superposition principle is not valid, the response may contain frequencies not present in the input, and system stability may depend on the excitation and the initial conditions. Therefore, techniques for the analysis of nonlinear systems are still in the early stages of development.

The describing function method grew out of attempts to extend the powerful transfer function concept of linear system analysis to cover nonlinear systems. It is a frequency-response technique rather

than a time-domain technique, the describing function being a type of equivalent frequency response function for a nonlinear element. The method is applied to systems in which the components of the loop can be separated into two parts, a nonlinear block followed by purely linear elements. Figure 1 illustrates such a system.

Assumptions of the method

The describing function method involves three basic assumptions. First, the system contains only one nonlinear element; second, the nonlinear characteristic does not change with time; and third, if the input to the nonlinearity is a sinusoid, only the fundamental component of its output is significant in returning via the feedback loop to the input. The third assumption demands that no significant subharmonic be generated by the nonlinear element. If this is granted, one justifies the third assumption, first by the fact that the harmonics in the output of the nonlinear element generally have smaller amplitude than the fundamental, and second by the fact that most linear components used in control systems (excluding compensators) have low-pass filter characteristics, so that the higher harmonics will be attenuated more than the fundamental in passing through the linear block.

Gille, Pélegrin, and Decaulne note that the vagueness with which the approximation to the first harmonic is justified is ". . . one of the weaknesses of the [describing function] method."[1]

---

[1] J-C Gille, M. J. Pélegrin, and P. Decaulne, Feedback Control Systems (New York: McGraw-Hill Book Company, Inc., 1959), p. 405.

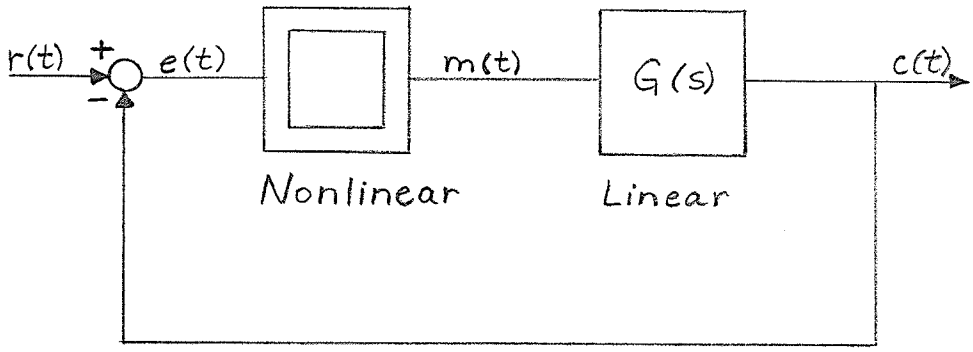

FIGURE 1

NONLINEAR FEEDBACK SYSTEM

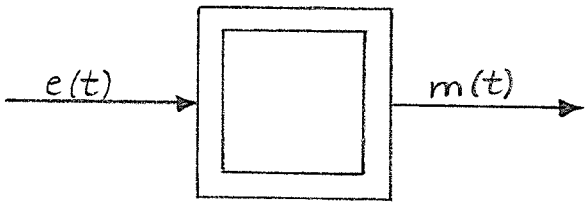

FIGURE 2

NONLINEAR ELEMENT

Definition of the describing function

Consider the nonlinear element shown in Figure 2. The conventional describing function is derived assuming a sinusoidal input $e(t) = E \sin wt$.[2] The response m(t) will be periodic but not sinusoidal, and expanded in a Fourier series will have the form

$$m(t) = M_1 \sin (wt + \phi_1) + M_2 \sin (2wt + \phi_2) + M_3 \sin (3wt + \phi_3) + \ldots \qquad (I - 1)$$

If the fundamental term $M_1 \sin (wt + \phi_1)$ is taken to be the "equivalent" of m(t), then an "equivalent transfer function" having magnitude M_1/E and phase ϕ_1 may be defined for the nonlinearity. Both the magnitude and phase will in general be functions of E and w,

$$\frac{M_1}{E} = B(E,w) \quad \text{and} \quad \phi_1 = \phi_1(E,w) \qquad (I - 2)$$

The "generalized transfer function" for the nonlinearity will then be of the form

$$N(E,w) = B(E,w) \underline{/\phi_1(E,w)} \qquad (I - 3)$$

It can be represented graphically as a family of transfer loci graduated in w, one locus for each value of E. If N is independent of the frequency w,[3] and depends only on the input amplitude E, it is called the "describing function" of the nonlinear element,[4]

$$\text{Describing function} = N(E) = B(E) \underline{/\phi_1(E)} \qquad (I - 4)$$

---

[2]The letter w will be used throughout this text in place of the Greek letter "omega", ω.

[3]This will be true if the nonlinear system does not contain any energy-storage elements.

[4]Some authors consider the describing function to be frequency dependent as well as amplitude dependent. The definition adopted here, however, follows that of Gille, Pélegrin, and Decaulne, op. cit., pp. 405-406.

The family of transfer loci may then be replaced by a single locus graduated in input amplitude.

The describing function thus arises from the concept of "quasi-linearization", in which the response of a nonlinear element to a given input is divided into two parts, the response of a linear element driven by that input, and an additional distortion component or "remnant". If the input is sinusoidal, the first part of the response, the fundamental, is characterized by the describing function of the element, which is simply the frequency response-function of the linearized nonlinear element. The output is then the sum of the describing function times the input and the remnant. Under the assumption of good low-pass filtering by the linear element of a system the distortion component is neglected in the analysis. The describing function is, then, only an approximation to the actual response characteristics of a nonlinear element.

Although in this investigation attention will be focused on the conventional sinusoidal input describing function, which represents the output of a nonlinearity by the fundamental component of its Fourier series, other sinusoidal input describing functions have been defined.[5] In addition to the sinusoidal input describing functions, two other types have been formulated, transient (or step) input and stationary random input describing functions.

---

[5]Robert R. Rankine, Jr., "An Evaluation of Selected Describing Functions of Control System Nonlinearities,"(report GGC/EE/64-16, Air Force Institute of Technology, Air University, United States Air Force, Wright-Patterson Air Force Base, Ohio, 1964), pp. 3-4.

The amplitude dependence of the describing function[6] reflects the nonlinear behaviour of an element. The describing function may be purely real, or it may contain a phase shift. It will be real in the case of a single-valued nonlinearity and complex for a double-valued nonlinearity, or a nonlinearity with memory.

Use of the method in analysis of autonomous and non-autonomous systems

The describing function approximation for a nonlinearity can be used to determine whether a self-sustained oscillation can exist in an autonomous (unforced) system ($r(t) \equiv o$ in Figure 1). The basic equation for this analysis, which is a sufficient condition for the existence of sustained oscillation, is

$$G(jw) = -\frac{1}{N(E)} \qquad (I - 5)$$

The $G(jw)$ and $-1/N(E)$ curves may be plotted in the complex plane, with w and E the running parameters respectively, and checked for an intersection. If such an intersection is found, the amplitude and frequency of the corresponding self-oscillation are determined from the $-1/N(E)$ and $G(jw)$ loci respectively at the intersection point. From the relative location of the two loci conclusions can be drawn about the stability of the autonomous system for various amplitudes at the input of the nonlinear element.

The describing function representation of a nonlinearity is also useful in finding the closed-loop frequency response of a non-

---

[6] From now on the term "describing function" will be taken to mean "conventional sinusoidal input describing function."

linear system to a sinusoidal forcing function. Consider the system diagram, Figure 1. For sinusoidal inputs,

$$e(jw) = E \sin (wt + \phi)$$

$$r(jw) = R \sin wt$$

$$G(s) = G(jw)$$

a closed-loop transfer function relating the error signal e(t) to the input may be written as

$$\frac{e(jw)}{r(jw)} = \frac{1}{1 + N(E)G(jw)} \qquad (I - 6)$$

From this a magnitude relationship

$$\frac{E}{R} = \left| \frac{1}{1 + N(E)G(jw)} \right| \qquad (I - 7)$$

is written. For a given G(jw) the relationship may be solved for N(E). The right hand side of the equation obtained will be a function of R, w, and E. If a fixed value of R is chosen, the right hand side can be plotted against E for various values of w. The left hand side, plotted against E, is just the describing function of the nonlinearity. Possible operating points are given by the intersections of the curves, and the values of E and w at these operating points are found from the diagram. With E known the magnitude of the system response c(t) can be found and plotted against w, the frequency of the forcing function, for the value of forcing function amplitude (R) chosen. More detailed discussions of the use of the describing function in analyzing closed-loop frequency response are given by Truxal[7] and Gibson[8].

---

[7]John G. Truxal, Automatic Feedback Control System Synthesis (New York: McGraw-Hill Book Company, Inc., 1955), pp. 581-585.

[8]John E. Gibson, Nonlinear Automatic Control (New York: McGraw-Hill Book Company, Inc., 1963), pp. 389-395.

Error involved in the method

The describing function method, being an approximation, involves a certain amount of error and uncertainty. According to Truxal,[9] an analysis based on describing functions involves three notable difficulties. Two of them are computational difficulties which can be remedied considerably with machine aids, while

> The third and most basic difficulty is related to the inaccuracy of the method and, in particular, to the uncertainty throughout the analysis about the accuracy. There is no simple method for evaluating the accuracy of the describing-function analysis of a nonlinear system and no definite assurance that the results derived with the describing function are even approximately correct.[10]

Johnson[11] has obtained correction terms for the amplitude and frequency of oscillation predicted by the describing function method. An important result of his analysis is that the first frequency correction term is zero. Therefore, the describing function frequency prediction is usually quite accurate. The first amplitude correction is non-zero, however, so the amplitude prediction is somewhat less accurate. Although Johnson's analysis gives an idea of the error in the describing function predictions and provides a means by which the accuracy of the predictions may be improved, it is of limited use to the engineer because of its computational complexity.

---

[9] Truxal, op. cit., pp. 599-601.

[10] Loc. cit.

[11] E. C. Johnson, "Sinusoidal Analysis of Feedback-Control Systems Containing Nonlinear Elements," Trans. AIEE, Vol.71, Part II. Applications and Industry, July, 1952, pp. 169-181.

For the describing function technique to be completely accurate, the linear element of the system must act as a perfect low-pass filter. In practical systems this will not be achieved, and some higher harmonics, although attenuated, will be fed back along with the fundamental to the input of the nonlinearity. Because of this, the describing function technique will tend to underestimate the amplitude of self-sustained oscillations. Rankine[12] observed that the accuracy of the describing function amplitude prediction decreased as the amplitude of the steady oscillation, or limit cycle, increased; that it decreased as the system order[13] decreased, giving poorer filtering; and that it seemed to vary with system type,[14] decreasing as the system type was increased. Graham and Hofmann[15] have commented on the lack of knowledge in many cases about the effect of neglecting the higher harmonics in the analysis. They have shown that the presence of a third harmonic[16] at the input to a nonlinearity can produce a substantial

---

[12]Rankine, op. cit., pp. 82-83.

[13]The "order" of a system is the number of poles minus the number of zeros in the linear transfer function.

[14]The "type" of a system refers to the multiplicity of the pole of the linear transfer function at s = o.

[15]Dunstan Graham and Lee Gregor Hofmann, "Investigations of Describing Function Technique," (Technical Report AFFDL-TR-65-137, Air Force Flight Dynamics Laboratory, Research and Technology Division, Air Force Systems Command, Wright-Patterson Air Force Base, Ohio, February, 1966), Chapters I and III.

[16]If the output of a nonlinearity is assumed to be odd symmetric, or half-wave symmetric, its Fourier series will contain no even harmonics. The third harmonic will then be the first harmonic above the fundamental.

phase lag in the fundamental component of the response. The prediction of limit cycle existence and limit cycle parameters (amplitude and frequency) can be notably affected by this phase shift. In fact, in systems for which the $-1/N(E)$ and $G(jw)$ curves intersect at a small angle, are tangent, or approach closely without intersecting, even small phase shifts in the fundamental due to the presence of higher harmonics can be of "crucial importance" in limit cycle prediction. In these cases results obtained from a describing function analysis must be viewed with suspicion.

It should not be assumed from the above remarks that the accuracy of the describing function analysis is necessarily poor. Graham and McRuer feel that the describing function approximation ". . . provides answers which are accurate to within 5 to 10% for a wide variety of systems. Results which are this close are ordinarily well within the probable accuracy of the mathematical description of the components."[17] Nevertheless, an element of doubt still remains about the accuracy of the method. According to Gille, Pélegrin, and Decaulne:

> . . . cases may arise in which the first-harmonic [describing function] approximation leads to incorrect results. . . . Fortunately most of these cases are examples that have been thought up on purpose. In any event, there is no sure criterion [italics in the original] that specifies under what conditions and within what limits the first-harmonic approximation can be applied safely. As a result, the method should be applied with great circumspection when studying systems with several degrees of freedom or when investigating the low-frequency behavior.[18]

---

[17] Dunstan Graham and Duane McRuer, Analysis of Nonlinear Control Systems (New York: John Wiley and Sons, Inc., 1961), p. 193.

[18] Gille, Pélegrin, and Decaulne, op. cit., p. 431.

Importance of the method

The describing function method is a valuable tool for the analysis of nonlinear feedback systems. Once the describing function has been found for a nonlinear element, that element can be treated as having a gain and phase shift varying with input amplitude. Keeping in mind that system stability must be analyzed as a function of input amplitude as well as frequency, one can employ the Nyquist diagram, the gain and phase plots, and all the usual frequency-response methods in the analysis and design of the nonlinear system. According to Graham and McRuer:

> Sinusoidal input describing functions . . . have a surpassing importance in the analysis of nonlinear control systems because they are particularly amenable to the determination of stability [italics in the original]. It has been repeatedly shown that their use produces good results with a modicum of effort. Furthermore, the use of sinusoidal input describing functions permits the extension to nonlinear control systems of the well-known harmonic or frequency response method of designing equalizing or compensating networks. This is a tremendous and almost unique advantage.[19]

Furthermore, the describing function technique may be applied to systems of any order. It is generally more accurate the higher the order of the system.

For a more complete discussion of the various aspects of the describing function method, the reader is referred to references (4), (5), (8), and (17) of the bibliography.

---

[19]Graham and McRuer, op. cit., p. 80.

II. THE PROBLEM

Statement of the problem

During the past few years considerable work has been done in an attempt to estimate the accuracy of predictions made using the describing function. The original purpose of this investigation was (1) to study several recent papers concerning describing function accuracy and perhaps deriving bounds on the amplitude and frequency of system response, both for autonomous and non-autonomous systems; (2) to apply the various bound expressions given in these papers to a selected set of systems and compare the results with the describing function amplitude and frequency predictions; and (3) if possible, from this comparison to state that for a certain type of system a certain author's bounds would be the best (i.e. tightest), while for another type of system another author's bounds would perhaps be better.

Importance of the study

As previously noted, the describing function technique is extremely useful to engineers engaged in the analysis and synthesis of nonlinear feedback systems. As also noted, however, the accuracy of the method is uncertain. It is therefore important from an engineering standpoint to try to improve the accuracy of the describing function method, to derive rigorous criteria which tell how accurate describing function predictions are, and to establish definite bounds on the parameters of system response. In this investigation an attempt was made to further some of the recent research done on these problems.

Chapter II gives a review of literature pertinent to this investigation.

CHAPTER II

REVIEW OF THE LITERATURE

Literature applying to autonomous systems

Quazza[1] considers the restricted class of autonomous systems whose nonlinear element is a relay with hysteresis. An example system is given for which the describing function method fails. No intersection of the G(jw) and -1/N(E) curves is found, yet the system oscillates. Corrections are proposed to (1) ensure the validity of the describing function method in cases where the number of zeros in the linear transfer function is equal, or lower by only one, to the number of poles; and (2) to improve the accuracy of the describing function amplitude and frequency predictions for those cases in (1) for which the attenuation of the linear element near the fundamental frequency of the response may be poor.

Rozenvasser[2] deals with the problem of determining periodic oscillations in control systems containing a single piecewise linear nonlinearity and reduces it to the determination of forced oscillations of a linear system with periodically changing parameters. From

---

[1] G. Quazza, "On the Validity of the Describing Function -, Tsypkin - and Hamel - Methods for the Study of Self Oscillations in On - Off Systems," Alta Frequenza, Vol. XXXII, No. 2, February, 1963, pp. 142-156.

[2] E. N. Rozenvasser, "On the Accurate Determination of Periodic Regimes in Sectionally Linear Automatic Control Systems," Automation and Remote Control, Vol.21, 1960, pp. 902-910.

the solution of an auxiliary Fredholm integral equation of the second kind, these forced oscillations may be found exactly. Both self - and forced oscillations of a steady-state nonlinear system are investigated. For the former case Rozenvasser derives estimates of the error incurred by approximating the exact solution in practical calculations.

Glatenok[3] considers the problem of the existence of periodic solutions of the differential equation $\ddot{y} = f(y,\dot{y})$ by means of the harmonic balance (describing function) method. He seeks to establish a range about the amplitude value predicted by the describing function, within which the amplitude of the exact periodic solution must lie. Three theorems are presented which, for different conditions on the function $f(y,\dot{y})$, give the existence of a stable periodic solution and the particular range within which its amplitude must lie. These theorems are not proved in Glatenok's article, although the basic idea behind the proofs is given. A system containing a backlash nonlinearity is discussed as an example. From the example it appears that Glatenok's technique produces a rather liberal range for the exact solution amplitude.

---

[3] I. V. Glatenok, "On the Foundation of the Harmonic Balance Method," Symposium on Nonlinear Vibrations, Kiev, U.S.S.R., September, 1961.

Garber and Rozenvasser,[4] combining forces in a joint publication, present a graphical procedure for estimating in the case of a self-oscillating system:

(1) the amplitude, A, of the first harmonic component of the actual system response in the form

$$A_\ell \leq A \leq A_h$$

and the oscillation frequency, w, in the form

$$w_\ell \leq w \leq w_h$$

(2) an upper bound on the peak magnitude of the response.

Literature applying to non-autonomous systems

Sandberg[5] studies the functional equation for a nonlinear feedback system $x = \underline{F}\psi[x + y]$, where $\underline{F}$ is a linear operator, ψ is the nonlinear function, y is the forcing function, and x is the response. He uses the contraction - mapping fixed - point theorem and other techniques of functional analysis to obtain, among other things, an upper bound on the mean-squared error that results when the describing function method is applied to the system.

The determination of steady-state forced periodic oscillations in nonlinear systems is considered by Garber.[6] The input to the non-

---

[4]E. D. Garber and E. N. Rozenvasser, "The Investigation of Periodic Regimes of Nonlinear Systems on the Basis of the Filter Hypothesis," Automation and Remote Control, Vol. 26, 1965, pp. 274-285.

[5]I. W. Sandberg, "On the Response of Nonlinear Control Systems to Periodic Input Signals," The Bell System Technical Journal, Vol. XLIII, No. 3, May, 1964, pp. 911-926.

[6]E. D. Garber, "Error Estimation in the Describing Function Method," Automation and Remote Control, Vol. 24, 1963, pp. 449-458.

linear element is obtained in integral equation form for the cases $D(o) \neq o$ and $D(o) = o$, where $D(p)$ is the denominator polynomial of the linear transfer function. Estimates of the error in the describing function solution are then derived for certain restrictions on the nonlinear characteristic. Garber gives an example system for which the error estimate is found. The derivation is extended to the case of an automatic optimizing system whose dynamics are described by equations with periodic coefficients.

As noted previously, Rozenvasser does some work involving the exact determination of forced periodic oscillations in systems having a single piecewise linear nonlinearity. Although in this case no error estimates are obtained for the describing function method, his work provides a basis for some of the ideas brought out in the joint Garber and Rozenvasser article referred to in the previous section.

For forced systems the joint Garber and Rozenvasser article gives estimates of the error in the describing function solution, of the type given by Garber. The estimates are again derived from the integral equation representation of the input to the nonlinear element. They are, however, supposed to be better than Garber's original estimates.

Three other references are mentioned at this point. Although they do not give any error estimates for describing function solutions, they nevertheless relate to the use of the method and contribute additional information about it.

Bass[7] gives a rigorous discussion of the mathematical validity of the describing function technique.

Hale[8] comments briefly on equivalent linearization and the describing function method.

In an article by Kislyakov, which is itself of little importance as far as this investigation is concerned, reference is made to the work of Khalanai.[9] According to Kislyakov, Khalanai proves the theorem, in providing ". . . the foundations of the averaging method [harmonic linearization method] as applied to systems of quasilinear differential equations with a lagging argument," that ". . . the error in determining the periodic solution of the averaged system is small compared to error in the periodic solution of the original system of differential equations with a lagging argument."[10] This probably means that the error in determining the periodic solution of the original system by using the averaged system is small; in other

---

[7]R. W. Bass, "Mathematical Legitimacy of Equivalent Linearization by Describing Functions," Proceedings of the First International Congress of the International Federation of Automatic Control (I.F.A.C.), Moscow, 1960 (London: Butterworths, 1961), pp. 895-905.

[8]Jack K. Hale, Oscillations in Nonlinear Systems (New York: McGraw-Hill Book Company, Inc., 1963), pp. 99-102.

[9]A. Khalanai, "Averaging method for systems of differential equations with a lagging argument," Revue de mathematiques pures et appliquees, Vol. 4, No. 3, 1959, cited by V. S. Kislyakov, "Foundations for the Application of the Harmonic Linearization Method to an Investigation of Periodic Oscillations in Systems with Lag," Automation and Remote Control, Vol. 21, 1960, pp. 1051-1056.

[10]Kislyakov, op. cit., p. 1053.

words, the averaged system is a good approximation. Khalanai's work was not pursued in this investigation.

Comments on the investigation

Several points were noted with regard to the articles applying to autonomous systems. Quazza's article applies only to a restricted class of nonlinear systems. Rozenvasser's article has been succeeded by the combined Garber - Rozenvasser article. Finally, the combined Garber - Rozenvasser article was published more recently than Glatenok's work. On the basis of these considerations it was decided to restrict the study of error estimates for autonomous systems to the combined Garber - Rozenvasser article.

For the study of non-autonomous systems, it was originally thought that the Sandberg, Garber, and combined Garber - Rozenvasser articles would provide a suitable selection of estimates. Study of the latter two articles, it was felt, would show how much the combined Garber - Rozenvasser estimates really improved upon Garber's original estimates.

The next step was to choose some suitable systems to which the various estimates could be applied. For the autonomous case the set of systems studied by Rankine[11] was selected. Rankine had obtained the experimental results for all his systems by simulating them on an analog computer, and the describing function[12] amplitude and frequency predictions were also given for each. It was felt that this was a typical

---

[11]Rankine, op. cit., 130 pp.

[12]The term "describing function" as used in this text is synonomous with Rankine's "conventional describing function."

set of systems and one for which, fortunately, the experimental results had already been determined, thus affording a substantial saving in work. The autonomous Garber - Rozenvasser estimates could, then, be applied to Rankine's systems in the first part of the investigation. For the non-autonomous study, it was thought that perhaps a few of the systems from the autonomous study, those for which the estimates had been best (i.e. most accurate) and worst (i.e. least accurate), could be investigated with their loop gains reduced. If necessary some other suitably-chosen forced systems could be studied.

The investigation began with the application of the Garber - Rozenvasser estimates for the autonomous case to Rankine's systems. Although, as indicated, the problem originally included both the autonomous and non-autonomous cases, sufficient work was subsequently found in the autonomous case, with the result that the non-autonomous estimates were not investigated any further. Therefore, since the work that follows involves the autonomous Garber - Rozenvasser estimates, a brief resumé of their derivation and application is given in the next section.

The Garber - Rozenvasser estimates

In Section 1 of their article, Garber and Rozenvasser comment briefly on previous investigations and problems associated with the estimation of the error in the describing function method. They consider the system

$$\left.\begin{aligned} x &= W(p)y + \phi = \frac{K(p)}{D(p)}\, y + \phi \\ y &= f(x) \end{aligned}\right\} \qquad (1.1)^{13}$$

[13] All equations, inequalities, or conditions numbered in this way, with two Arabic numerals separated by a decimal point, are those given in the Garber - Rozenvasser article.

which is represented in Figure 3. $W(p) = K(p)/D(p)$ is the linear element transfer function, with $K(p)$ of lower degree than $D(p)$, $\phi(t)$ is a periodic forcing function at frequency w, $x(t)$ is the input to the nonlinear element, and y is its output. The nonlinearity $f(x)$ is assumed piecewise continuous and ". . . such that regimes $x(t)$, symmetric and periodic in the frequency w, are possible in the system. . . ."[14] For $x(t)$ the integral equation form

$$x(t) = \int_0^{T/2} \bar{\phi}(t-\tau)\, f[x(\tau)]\, d\tau + \phi(t) \qquad (1.3)$$

is written, the kernel $\bar{\phi}(t-\tau)$ being the Fourier series

$$\bar{\phi}(t-\tau) = \frac{w}{\pi} \sum_{s=-\infty}^{\infty} W[(2s+1)iw]\, e^{(2s+1)iw(t-\tau)} \qquad (1.4)$$

Closed forms for the kernel are given for the case in which the equation $D(\lambda) = 0$ has simple roots.

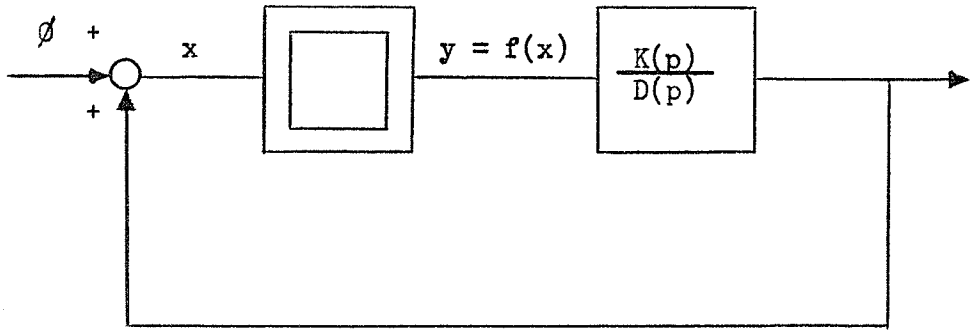

FIGURE 3

GARBER-ROZENVASSER FEEDBACK SYSTEM

Section 2 deals with the estimates for non-autonomous systems and

---

[14] Garber and Rozenvasser, op. cit., p. 275.

hence does not apply directly to this discussion. However, that portion of the section dealing with the estimation of the parameter I(w) defined by the equation

$$I = \int_o^{T/2} \left|\dot{\phi}(u)\right| \, du \tag{2.6}$$

is important to the autonomous case. A bound on I(w), expressed by the relation

$$I(w) \leq \bar{I}(w) = \sqrt{2 \sum_{s=o}^{\infty} \left| W[(2s+1)iw] \right|^2} \tag{2.11}$$

is derived using the Bunyakovskii inequality[15] and Parseval's formula. The following expression for the bound, which contains a finite sum over the roots of the equation $D(\lambda) = o$, is then obtained:

$$\bar{I}(w) = \sqrt{\frac{\pi}{w} \sum_{\rho=1}^{n} \frac{K(\lambda_\rho)\, K(-\lambda_\rho)}{D'(\lambda_\rho)\, D(-\lambda_\rho)} \tanh \left(\frac{-\pi \lambda_\rho}{2w} \right)} \tag{2.13}$$

Section 3 begins the derivation of error estimates for autonomous systems ($\phi \equiv o$ in equations (1.1)). In this case w, the frequency of the oscillation, is not known a priori as it is for a forced system, so that estimates of the type derived for forced systems cannot be used. Garber and Rozenvasser write x(t) as a sum, $x(t) = x_1(t) + x_h(t)$, $x_1(t)$ being the fundamental component and $x_h(t)$ the sum of the higher harmonics. The two integral equation forms

---

[15] According to Nicholas D. Kazarinoff, Analytic Inequalities (New York: Holt, Rinehart and Winston, 1961), pp. 71-72, this is what Western writers commonly know as Schwarz's Inequality, although Bunyakovskii obtained the result earlier than Schwarz.

$$x_1(t) = \int_0^{T/2} \phi_1(t-\tau)\, f[x(\tau)]\, d\tau \qquad (3.3)$$

and

$$x_h(t) = \int_0^{T/2} \phi_h(t-\tau)\, f[x(\tau)]\, d\tau \qquad (3.4)$$

replace equation (1.3), $\phi_1(t-\tau)$ and $\phi_h(t-\tau)$ being respectively the fundamental component and the sum of the higher harmonics of the kernel $\phi(t-\tau)$. Without loss of generality $x_1(t)$ is assumed to have the sinusoidal form $x_1(t) = A \sin wt$. By substitution and algebraic manipulation of equation (3.3) they obtain the result

$$W(iw)\, R(A,x_h) = 1 \qquad (3.6)$$

where $R(A,x_h)$ is given by the relation

$$R(A,x_h) = \frac{2w}{\pi A} \int_0^{T/2} f[A \sin wt + x_h(t)]\, (\sin wt + i \cos wt)\, dt \qquad (3.7)$$

Equation (3.6) is similar to the fundamental equation of the describing function method (noting that system (1.1) is a positive feedback system), viz., equation (I - 5) on page 6, and does in fact become the fundamental equation when $x_h(t) \equiv o$, $R(A,o)$ being just the describing function of the nonlinear element. If $x_h(t)$ is known, the process of equating real and imaginary parts of both sides of (3.6) yields two equations for the two unknowns A and w. If $x_h(t) \equiv o$, (3.6) has the solution A_b, w_b which is that obtained by the describing function method. To estimate the differences between A and A_b and w and w_b, one must estimate $|x_h(t)|$.

In Section 4 Garber and Rozenvasser deal with the estimation of $\Delta = \max |x_h(t)|$ using equation (3.4) and making extra assumptions on f(x). First, for f(x) satisfying (4.1), viz., $|f(x)| \leq N = \text{const.}$, they derive the bound on Δ in the form

$$\Delta \leq N\, \epsilon(w) \qquad (4.3)$$

The parameter $\varepsilon(w)$ is defined by the equation

$$\varepsilon(w) = \int_0^{T/2} \left| \phi_h(u) \right| \, du \tag{4.4}$$

where the w-dependence enters through the T/2 upper limit on the integral. Second, for f(x) satisfying (4.5), viz., $|f(x)| \leq M_o |x|$ (M_o = const.), they obtain under the condition

$$1 - M_o \varepsilon(w) > o \tag{4.7}$$

the inequality

$$\Delta \leq \frac{AM_o \, \varepsilon(w)}{1 - M_o \varepsilon(w)} \tag{4.8}$$

Finally, f(x) is assumed piecewise differentiable and of finite slope bounded in magnitude by the constant M_1. Equation (3.4) is integrated by parts to introduce the slope of the nonlinear function. Straightforward manipulation yields the inequality

$$\Delta \leq \frac{M_1 \, A \, w \, \varepsilon^*(w)}{1 - M_1 \, \varepsilon(w)} \tag{4.18}$$

with its required extra condition

$$1 - M_1 \, \varepsilon(w) > o \tag{4.17}$$

The parameter $\varepsilon^*(w)$ is given by the equation

$$\varepsilon^*(w) = \int_0^{T/2} \left| \phi_h{}^*(u) \right| \, du \tag{4.13}$$

where the function $\phi_h{}^*$ is defined by the relation

$$\phi_h{}^*(t-\tau) = -\frac{1}{\pi} \sum_{\substack{s=-\infty \\ \left(\neq o \atop \neq -1\right)}}^{\infty} \frac{W[(2s+1)iw]}{(2s+1)i} \, e^{(2s+1)iw(t-\tau)} \tag{4.11}$$

Bounds on $\varepsilon(w)$ and $\varepsilon^*(w)$ given by the inequalities

$$\varepsilon(w) \leq \sqrt{2 \sum_{s=1}^{\infty} \left| W[(2s+1)iw] \right|^2} \tag{4.19}$$

and

$$\varepsilon^*(w) \leq \sqrt{2 \sum_{s=1}^{\infty} \frac{\left| W[(2s+1)iw] \right|^2}{(2s+1)^2 w^2}} \tag{4.20}$$

are derived in exactly the same way as the bound $\bar{I}(w)$ was derived for $I(w)$ in Section 2, using the Bunyakovskii inequality and Parseval's formula. The authors note that small values of $\varepsilon(w)$ and $\varepsilon^*(w)$ imply a small bound on Δ and hence good accuracy for the describing function predictions. Also, $\varepsilon(w)$ and $\varepsilon^*(w)$ depend on the filtration properties of the linear element of the system and decrease rapidly as w increases.

Garber and Rozenvasser obtain, in Section 5, their graphical procedure for finding bounds on the parameters of the response. They write equation (3.6) in the form

$$\frac{1}{W(iw)} - R(A,o) = R(A,x_h) - R(A,o) \tag{5.1}$$

and from the definition of $R(A,x_h)$, equation (3.7), write an expression for the right hand side, which is thought of as a vector ΔR. An expression is found for the projection of ΔR along a direction defined by an angle ψ from the vertical. Assumptions must now be made about the form of $f(x)$, and the function is assumed to satisfy the third condition of Section 4, that is to be piecewise differentiable with $|f'(x)| \leq M_1 = \text{const}$. Using the corresponding inequality (4.18) for the bound on Δ, they derive the inequality

$$|\Delta R_\psi| \leq \frac{4M_1^2 \, w \, \varepsilon^*(w)}{\pi[1 - M_1 \, \varepsilon(w)]} = \delta(w) \tag{5.5}$$

giving a bound $\delta(w)$ on the length of the projection of vector ΔR along the direction ψ. The fact that this bound is independent of ψ enables the authors to deduce that the lengths of both the real (horizontal) and imaginary (vertical) components of ΔR are bounded by $\delta(w)$. This idea is expressed by the following two inequalities:

$$|\text{Re } \Delta R| = \left|\text{Re}\left[\frac{1}{W(iw)} - R(A,o)\right]\right| \leq \delta(w) \tag{5.6}$$

$$|\text{Im } \Delta R| = \left|\text{Im}\left[\frac{1}{W(iw)} - R(A,o)\right]\right| \leq \delta(w) \tag{5.7}$$

These may be solved to give estimates of A and w, and form, in effect, a generalization of the describing function method. The estimates, however, are only valid for frequencies satisfying condition (4.17).

The right hand sides of inequalities (5.6) and (5.7) are independent of A. This makes possible a graphical procedure for finding the estimates of A and w which generalizes that followed in the describing function approach. The $1/W(iw)$ and $R(A,o)$ loci, or respectively the inverse Nyquist and describing function loci, are drawn in the complex plane. Their intersections give the describing function solutions A_b, w_b. Now the vector difference between the two loci must lie in a circle of radius $\delta(w)$. That is, $1/W(iw)$ is a function of w only, while $R(A,o)$ is a function of A only. For any possible A, w combination, the loci cannot differ by more than $\delta(w)$. Other combinations are impossible. At each value of w along $1/W(iw)$ a circle of radius $\delta(w)$, computed from (5.5), (4.19), and (4.20), is drawn, and the envelopes of these circles are constructed. The portion of $R(A,o)$ between the two envelopes provides the estimate of A in the form $A_\ell \leq A \leq A_h$. The frequency range

lies between the centres of circles tangent to R(A,o) and has the form $w_\ell \leq w \leq w_h$. Figure 1 of the article illustrates the procedure.

Garber and Rozenvasser finally obtain the bound on $|x_h(t)|$

$$|x_h(t)| \leq M_1 A_h \max_{w_\ell \leq w \leq w_h} \frac{w\,\varepsilon^*(w)}{1 - M_1\,\varepsilon(w)} \qquad (5.10)$$

by taking the maximum value of the right hand side of inequality (4.18) over the allowable ranges of A and w. This involves the use of A_h, the maximum allowable value of A, and the maximization of that part of the bound that depends only on w, $\frac{w\,\varepsilon^*(w)}{1 - M_1\,\varepsilon(w)}$, over the allowable range of w.

At the end of the section the comment is made that the method can be extended to non-autonomous systems.

Section 6 of the article contains two illustrative examples, a non-autonomous and an autonomous system. The autonomous example, which is of interest here, involves the system $(p^2 + 0.8p + 8)\,x = p\,f(x)$, where f(x) is a saturation of unit slope. One noteworthy point regarding this example is that in the final step the authors obtain a bound on the maximum possible magnitude of x(t), the input to the nonlinearity, which in the autonomous case is just the system response. This bound is derived from the equation $x(t) = A \sin wt + x_h(t)$ and involves the sum of A_h and the previously calculated bound on $|x_h(t)|$.

Chapter III outlines the procedure followed in applying the autonomous Garber - Rozenvasser estimates to Rankine's systems. A preview of the organization of the investigation is also given.

CHAPTER III

PROCEDURE FOLLOWED IN THE INVESTIGATION

The Garber - Rozenvasser autonomous system is described by the equation $x = W(p)y$, while Rankine's autonomous systems have the equation $x = -G(p)y$.[1] It is evident, therefore, that the $W(p)$ used in the Garber - Rozenvasser procedure will be the negative of Rankine's linear transfer function. In transform notation, $W(s) = -G(s)$.

The first step in applying the Garber - Rozenvasser estimates is to draw the $1/W(jw)$ [2] and $R(A,o)$ loci. For the given Rankine system with linear element $G(s)$, $-1/G(jw)$ was calculated in complex form. The real and imaginary parts of the expression were then evaluated by means of a digital computer for w-values in increments of 0.1 rad./sec. from zero up to some value determined by the size of the graph being drawn. The corresponding points were plotted in the complex plane on a suitable scale and joined to give the $1/W(jw)$ locus. Next, the $R(A,o)$ locus was drawn on the diagram. Since, as it turned out, only systems involving saturation and dead zone nonlinearities were investigated, this locus was easily drawn in each case. Since Rankine's saturation nonlinearity had a slope of 0.5, [3] its

---

[1] Rankine, op. cit., p. 11, Figure 1(b).

[2] Although Garber and Rozenvasser use "i" in the complex number notation, "j" will be used throughout this text.

[3] Rankine, op. cit. In the diagram on page 29 the slope of the saturation nonlinearity is denoted by K, while on page 36 it is noted that K was chosen to be 0.5.

describing function locus extended from 0 out to 0.5 along the positive real axis. The dead zone nonlinearity had a slope of 0.5 also,[4] so that its describing function locus was the same. Note that each point along the describing function locus for a nonlinearity corresponds to a certain input amplitude or range of input amplitudes.

The next step is to compute $\delta(w)$ at points along the $1/W(jw)$ locus. This involves first a computation of $\varepsilon(w)$ and $\varepsilon^*(w)$ using inequalities (4.19) and (4.20). These inequalities were put into their particular form for the given example by letting $(2s + 1) = k$, finding $W(jkw) = - G(jkw)$, and from it deriving the expression for $2\,|W(jkw)|^2$. A sum of this expression over $k = 3, 5, 7, \ldots$ replaced the sum over s in inequality (4.19). The expression was then divided by k^2w^2 and the result summed over $k = 3, 5, 7, \ldots$ to obtain the inequality for $\varepsilon^*(w)$. In this form the right hand sides of the two inequalities could easily be computed digitally.

For a particular value of w, $\varepsilon(w)$ was found by computing the successive terms in the series ($k = 3$, $k = 5$, $k = 7$, . . .) and summing them until the terms became less than 10^{-7} of the sum to that point. There the series was cut off and $\varepsilon(w)$ computed by taking the square root of the calculated sum. For the systems studied the procedure generally required the computation of approximately twenty to thirty terms in the series.

---

[4] Ibid. In the diagram on page 28 the dead zone nonlinearity has slope K, while on page 74 K is taken to be 0.5.

Once $\varepsilon(w)$ had been evaluated, condition (4.17) was checked. If it did not hold, the calculation proceeded to the next higher value of w. If the condition held, $\varepsilon^*(w)$ was computed by dividing each of the terms in the series for $\varepsilon(w)$ by k^2w^2, summing, and taking the square root, it being recognized that for $w > \frac{1}{3}$ the $\varepsilon^*(w)$ series will converge faster than the $\varepsilon(w)$ series. In accordance, the calculation of $\varepsilon(w)$ was only carried out for the w-values from 0.4 on. In every case studied, however, condition (4.17) did not hold at w = 0.4, and some larger w-value was found at which and beyond which the condition held. Hence in all the cases for which $\varepsilon^*(w)$ was computed, w was in fact larger than one third.

It will be noted that $\varepsilon(w)$ and $\varepsilon^*(w)$ have been found by evaluating the right hand sides of inequalities (4.19) and (4.20), so that these values are in fact the maximum ones that $\varepsilon(w)$ and $\varepsilon^*(w)$ can have. From (5.5) it is evident that they will in turn give the maximum $\delta(w)$ value, which is required for making proper estimates.

For the w-values satisfying condition (4.17), $\delta(w)$ was computed from relation (5.5). Circles of radius $\delta(w)$ were then drawn at the corresponding points on the $1/W(jw)$ locus, and the two envelopes of the circles were drawn. The estimates of A and w were found from the diagram in the forms $A_\ell \leq A \leq A_h$ and $w_\ell \leq w \leq w_h$. The value of A corresponding to a given point on the describing function locus was determined graphically from the appropriate curve given in Rankine's thesis. For example, for the saturation nonlinearity, X, which is equivalent to A used here, can be found for a given point N on the describing function

plot using curve 4 on page 38, K and S being known parameters for the nonlinearity.

The bound on $|x_h(t)|$ was found next. It was observed that in (5.10), using the definition of $\delta(w)$ in (5.5),

$$\frac{w\,\varepsilon^*(w)}{1 - M_1\,\varepsilon(w)} = \frac{\pi\,\delta(w)}{4M_1^2} \qquad \text{(III - 1)}$$

Therefore, (5.10) may be written as

$$|x_h(t)| \leq M_1 A_h \max_{w_\ell \leq w \leq w_h} \frac{\pi}{4M_1^2} \cdot \delta(w)$$

or

$$|x_h(t)| \leq \frac{\pi A_h}{4M_1} \max_{w_\ell \leq w \leq w_h} \delta(w) \qquad \text{(III - 2)}$$

It would be suspected that, since $\varepsilon(w)$ and $\varepsilon^*(w)$ ". . . decrease rapidly with increasing frequency,"[5] as w increases their decrease should offset the increase due to the factor w in the numerator of $\delta(w)$, with the net result that $\delta(w)$ should decrease with increasing frequency. This behaviour was indeed observed in every example studied. Therefore, the maximum of $\delta(w)$ over the range of w occurred at w_ℓ. Accordingly, the bound on $|x_h(t)|$ was computed from

$$|x_h(t)| \leq \frac{\pi A_h}{4M_1}\,\delta(w_\ell) \qquad \text{(III - 3)}$$

Finally, to complete the procedure the bound on the maximum magnitude of x(t) was determined by adding A_h and the calculated bound on $|x_h(t)|$. This bound and the frequency estimate could then be compared to the describing function amplitude and frequency predictions

---

[5] Garber and Rozenvasser, op. cit., p. 282.

found from the intersection of the $1/W(jw)$ and describing function loci.

Chapter IV describes the difficulties encountered when the Garber - Rozenvasser estimates were first applied to Rankine's systems, a check of Garber and Rozenvasser's autonomous example, and some attempts made to overcome the difficulties. Chapter V involves an attempt to improve the estimates by a "shift of gain" procedure, while in Chapter VI the estimates are applied to some hypothetical cases. Experimental results are compared to calculated results in Chapter VII. Chapter VIII deals with the plotting of an "A - w diagram" for different types of systems, while the conclusions of the investigation and recommendations for future work are given in Chapter IX.

CHAPTER IV

INITIAL DIFFICULTIES WITH THE AUTONOMOUS GARBER - ROZENVASSER ESTIMATES

I. APPLICATION OF ESTIMATES TO RANKINE'S SYSTEMS

The Garber - Rozenvasser estimates for the autonomous case were applied to selected systems from Rankine's set. The systems chosen were Rankine's seven saturation systems, involving linear elements $G_1(s)$ to $G_6(s)$ and $G_{3A}(s)$, the saturation nonlinearity being a convenient one which is piecewise differentiable and for which condition (4.9) holds. However, the technique failed in each case. The first three systems, containing linear elements $G_1(s)$ to $G_3(s)$, gave only right hand (low amplitude) intersections of the envelope with the describing function plot, as shown in Figure 4. The circles increased too rapidly in size, and the $1/W(jw)$ locus did not "dip" low enough below the describing function, with the result that a left hand intersection could not be obtained. For the other four systems no intersections of the envelope and the describing function were found, again because of too rapid an increase in the size of the circles. Figure 5 illustrates the situation.

The method was then applied to Rankine's first dead zone system (linearity $G_7(s)$), but no intersections were found for this case either. The situation was similar to that illustrated by Figure 4, except that

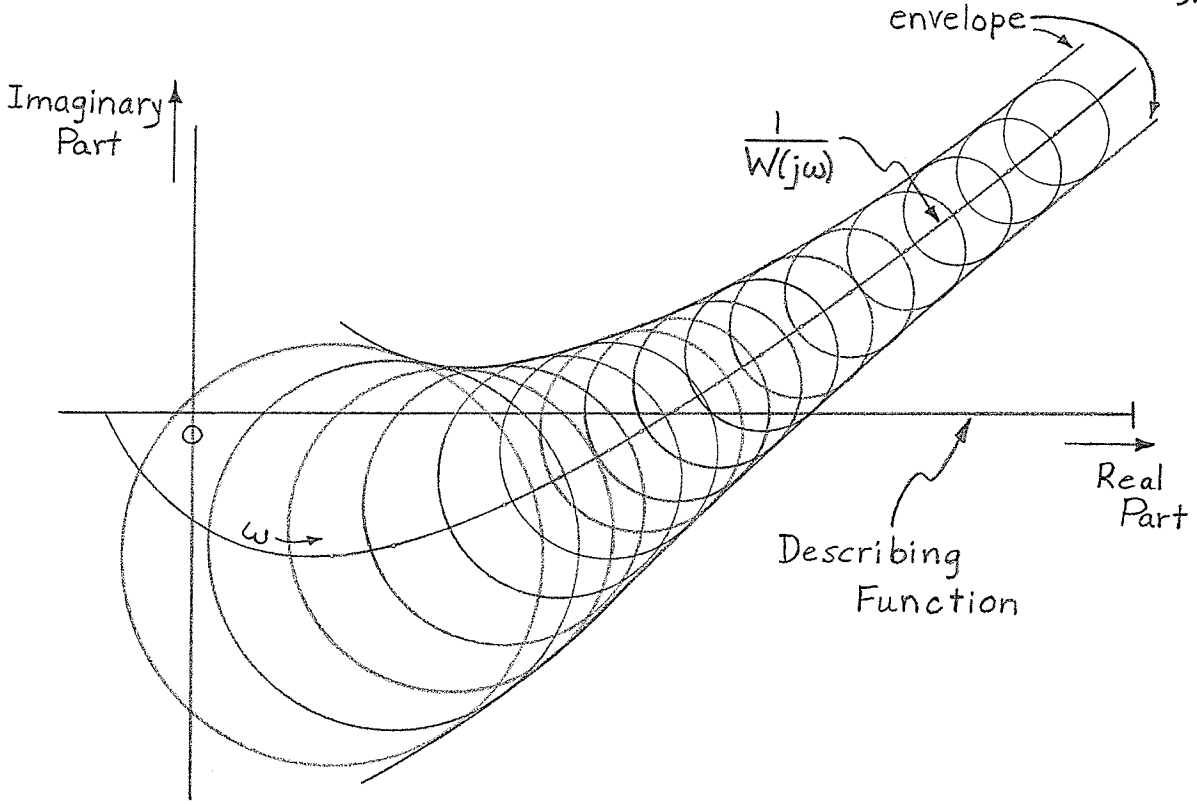

FIGURE 4

CASE WHERE ONLY RIGHT HAND ENVELOPE INTERSECTION AVAILABLE

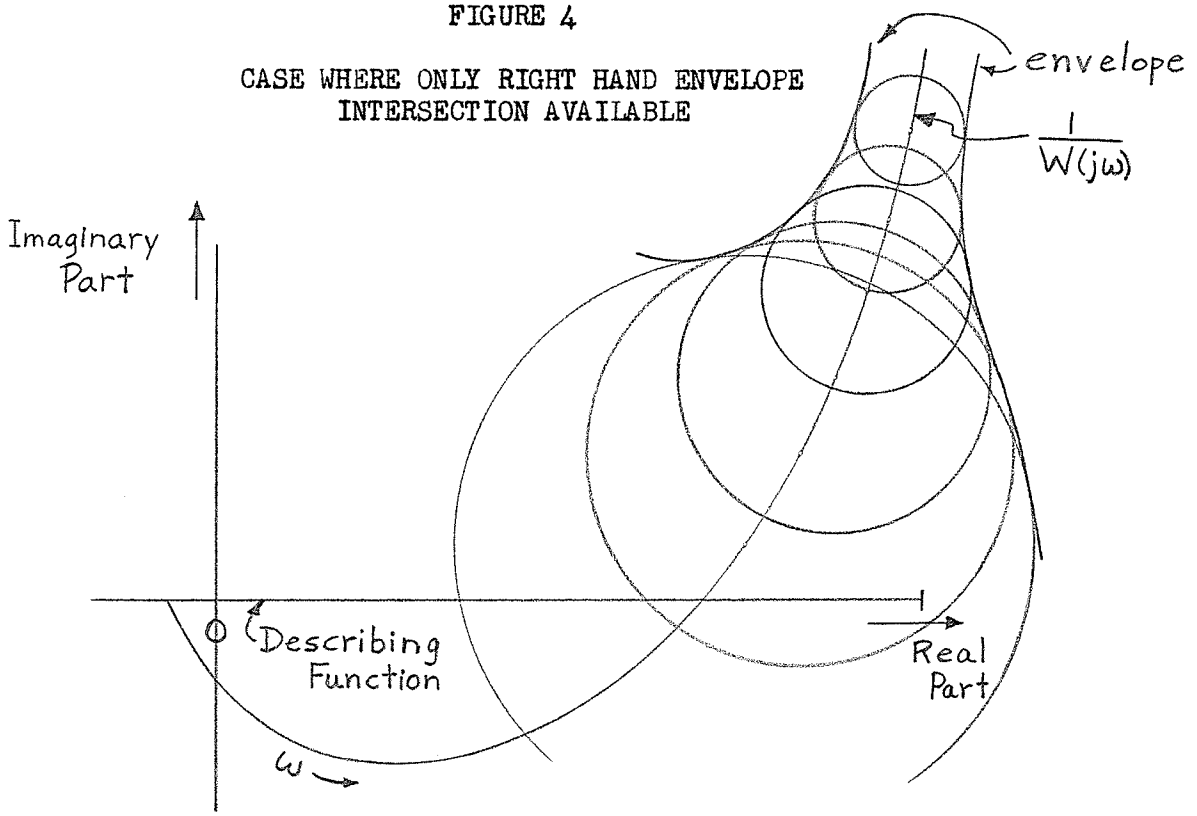

FIGURE 5

CASE WHERE NO ENVELOPE INTERSECTIONS AVAILABLE

the right hand envelope crossed beyond the end of the describing function.

It was observed that since $\varepsilon(w)$ and $\varepsilon^*(w)$ depend only upon the linear part of the system, they will be fixed for a given linear element. Hence if the linear element is not changed, but M_1 is increased, then $\delta(w)$ will increase correspondingly, while the $1/W(jw)$ locus will remain the same. It is evident, then, that if the technique fails in the first case it will also fail in the case where M_1 is increased. From this reasoning it was noted that the failure of the technique for Rankine's seven saturation systems also implied that it would fail for his seven systems involving saturation combined with dead zone, M_1 being 0.5 for his saturation nonlinearity and 1.0 for the saturation with dead zone nonlinearity.

Furthermore, increasing the gain of the linear element causes $\varepsilon(w)$ and $\varepsilon^*(w)$ to increase. For fixed M_1 this will result in an increase in $\delta(w)$. Since the larger gain appears in the denominator of $1/W(jw)$, points on the $1/W(jw)$ locus will lie closer to the origin, resulting in a general "moving in" of the locus toward the origin, as illustrated in Figure 6. It is again evident that the failure of the technique for Rankine's first dead zone system indicates that it will also fail when applied to his second dead zone system (linearity $G_{7A}(s)$).

In each of the cases to which the technique was applied it was observed that, as circles were drawn for decreasing values of w along the $1/W(jw)$ locus, an w-value was reached for which the circle would

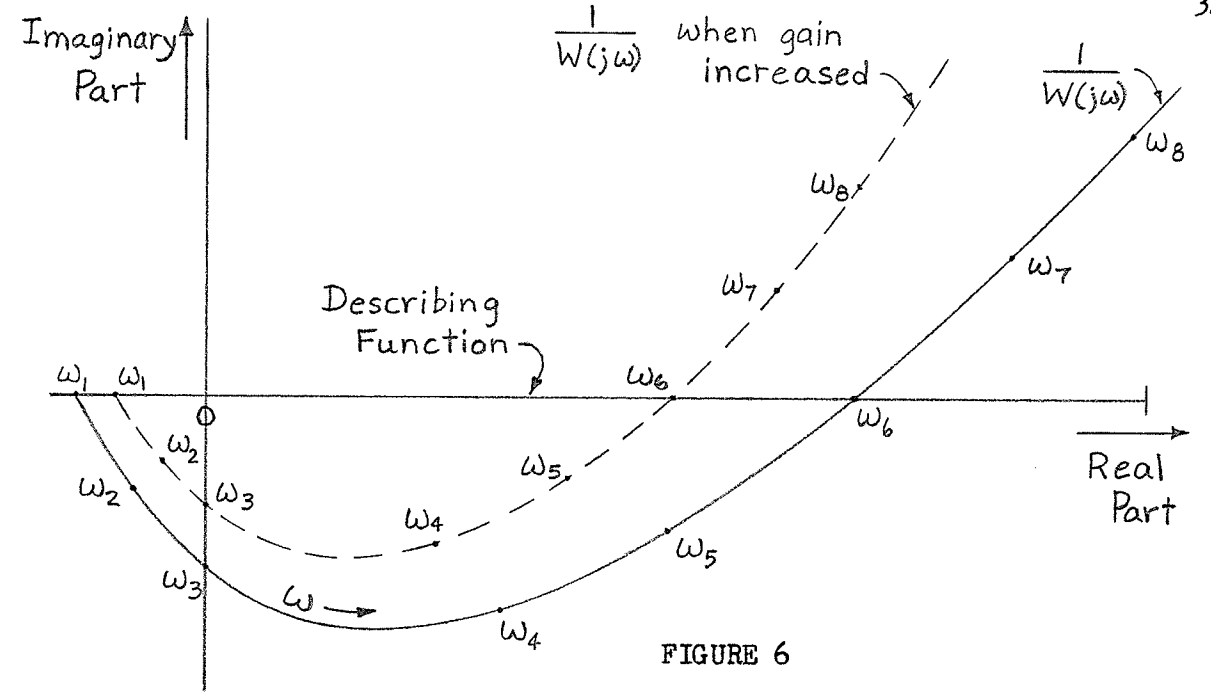

FIGURE 6

"MOVING IN" OF 1/W(jw) LOCUS
AS GAIN INCREASED

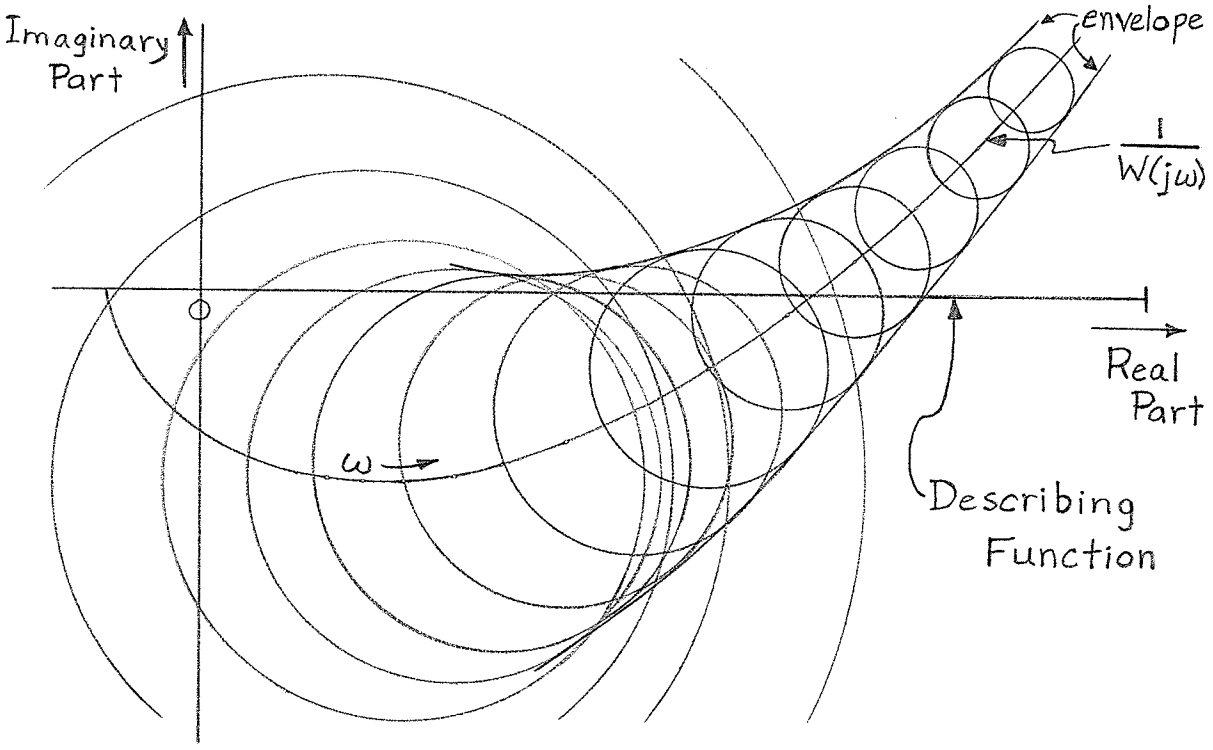

FIGURE 7

DOUBLING BACK OF ENVELOPE

completely enclose the previous circle. For subsequent values of w the circles would continue to increase rapidly in size, giving what appeared to be a doubling back of the envelope, as shown in Figure 7. This behaviour suggested the possibility of a second pair of intersections of the envelope and the describing function (in cases where the technique could be made to work -- that is, to give a first pair of intersections).

At this point it was decided to check the authors' second (autonomous) example in Section 6 for the possibility of a doubling back of the envelope and also to select one of the systems studied above and attempt to modify it so that the Garber - Rozenvasser technique could be made to work for that system.

II. CHECK OF SECOND GARBER - ROZENVASSER EXAMPLE

The method was applied to the authors' second example. The values of $\varepsilon(w)$ and $\varepsilon^*(w)$ were calculated using the series method of inequalities (4.19) and (4.20) as outlined in Chapter III. It was found, however, that the series for $\varepsilon(w)$ converged slowly for this low order W(s). Approximately 2100 to 3200 terms in the series were required before the terms reached 10^{-7} of the sum, the accuracy specified, for the w-values to be plotted. It was thought that perhaps, due to the slow convergence, a large number of terms after cutoff might produce an appreciable change in $\delta(w)$. Therefore, a check, it was thought, to

ensure that $\delta(w)$ values were being calculated accurately would be a good idea.

By means of results derived from equation (2.13), $\varepsilon(w)$ and $\varepsilon^*(w)$ were found in closed form rather than as an infinite series. From them the exact values of $\delta(w)$ were computed for the w-values to be plotted. Agreement between the exact $\delta(w)$'s and the approximate $\delta(w)$'s was so close that the plotting was totally unaffected. The details of the foregoing procedure are given in Appendix A.

Table I compares the results obtained in the check of this example to those obtained by Garber and Rozenvasser.

TABLE I

COMPARISON OF RESULTS FOR GARBER - ROZENVASSER EXAMPLE

Item	Results obtained in check	Results obtained by Garber and Rozenvasser
Amplitude range	$1.19 \leq A \leq 1.76$	$1.23 \leq A \leq 1.85$
Frequency range	$2.77 \leq w \leq 2.89$	$2.75 \leq w \leq 2.90$
Describing function predictions	$A_b = 1.45$ $w_b = 2.83$	$A_b = 1.55$ $w_b = 2.82$
Bound on $\lvert x_h \rvert$	$\lvert x_h \rvert \leq 0.165$ (use 0.17)	$\lvert x_h \rvert \leq 0.29$
Bound on max $\lvert x \rvert$	max $\lvert x \rvert \leq 1.93$	max $\lvert x \rvert \leq 2.14$

The authors' diagram (Figure 4 of their article) shows intersections of the $1/W(jw)$ locus and the describing function at 0.65 and 0.95. Using Rankine's describing function plot for the saturation nonlinearity[1] $A_h = 1.87$ is obtained from the 0.65 intersection and $A_\ell = 1.11$ from the 0.95 intersection. Their value of $A_\ell = 1.23$ seems to be in error, since it requires a right hand intersection at 0.90, which is impossible from the diagram. Their value of $w_\ell = 2.75$ seems plausible enough, but from Figure 4 $w_h = 2.90$ is impossible, since the $w = 2.90$ circle extends below the describing function. According to the diagram w_h should be about 2.92. Furthermore, in the describing function solution A_b should be 1.45 instead of 1.55. The authors' bound on $|x_h|$ seems larger than necessary, since a $\delta(w_\ell) = \delta(2.75)$ value of 0.20 is required to obtain a bound of 0.29, while from Figure 3 of their article $\delta(2.75)$ appears to be about 0.16, which would give a bound of 0.23 on $|x_h|$. Hence their bound on max $|x|$ is probably larger than necessary. It would appear that the bound should be 2.08 rather than 2.14. In summary, both the amplitude range and the frequency range appear to have been made narrower than they should be according to their diagrams, while the bounds on $|x_h|$ and max $|x|$ appear to be too liberal. The authors' value of A_b is in error.

Garber and Rozenvasser state that condition (4.17) is satisfied for $w > 1.15$. In the check a result of $w \geq 1.21$ was obtained.

---

[1] Rankine, op. cit., curve 4 on page 38.

Table II compares several $\delta(w)$ values obtained by the authors to those calculated in the check of the example.

TABLE II

COMPARISON OF SOME $\delta(w)$ VALUES FROM GARBER - ROZENVASSER EXAMPLE AND CORRESPONDING VALUES OBTAINED IN CHECK

w(rad./sec.)	Authors' value of $\delta(w)$	Value of $\delta(w)$ obtained in check
1.5	0.57	0.570
2.0	0.295	0.223
2.5	0.19	0.142
3.0	0.13	0.105
3.5	0.10	0.083
4.0	0.075	0.069
4.5	0.06	0.060
5.0	0.05	0.052

The $\delta(w)$'s found in the check are smaller than those of the authors in the range from w = 1.5 to w = 4.5. This results in a narrower envelope, giving tighter bounds on A and w, and in turn producing smaller bounds on $|x_h|$ and max $|x|$.

With regard to the possibility of a double envelope in this example, it was found that the circle drawn at w = 1.23 was so large that it completely enclosed the describing function, while that drawn at w = 1.24 lay entirely below the describing function. It was reasoned that, because of the continuity of the $\delta(w)$ graph, there must be some w between 1.23 and 1.24 for which condition (4.17) is satisfied and for which the circle cuts the describing function in two places. Hence the authors' example does exhibit a doubling back of the envelope as w decreases. However, the authors have used only the first part of the envelope in making their estimates for this system. This, it was felt, is sufficient justification for doing the same if and when a system is found for which the technique works.

III. ATTEMPTS TO MAKE GARBER - ROZENVASSER TECHNIQUE WORK

It was decided to work with the system involving the saturation nonlinearity and linear element $G_1(s)$ and attempt to modify it so that the Garber - Rozenvasser technique would work. To accomplish this $\delta(w)$ would have to be reduced so that two intersections could be obtained. It was decided for simplicity to try to modify the linear element and the nonlinear element separately, rather than modifying both together. The two possibilities chosen were:

(1) Leave the nonlinearity the same and lower the gain of the linear element. Thus M_1 will remain the same, while $\mathcal{E}^*(w)$ and $\mathcal{E}(w)$ will decrease, producing a decrease in $\delta(w)$. Also, condition (4.17) will hold for lower values of w.

(2) Leave the linear element the same and lower M_1, the linear range slope of the nonlinearity. Thus $\epsilon^*(w)$ and $\epsilon(w)$ will remain the same, while the reduction in M_1 will produce a decrease in $\delta(w)$. Condition (4.17) will again hold for lower w-values.

If the first possibility is followed, however, it is evident that as the linear element gain is reduced, the real and imaginary parts of points on the $1/W(jw)$ locus also increase, resulting in a "moving out" of the locus (the opposite situation to that depicted in Figure 6). If the gain is reduced too much, the $1/W(jw)$ locus will no longer intersect the describing function. Thus a compromise is necessary to make $\delta(w)$ as small as possible, while still ensuring that the two loci intersect.

The gain of $G_1(s)$ was reduced from its original value of 180 to 130, M_1 being left at 0.5, and the method was applied to this new system. The method worked, two intersections were found, and estimates of the parameters were calculated. The results are given in one column of Table III. As an example, the calculation procedure for this system is outlined in detail in Appendix B.

Following possibility (2) above, one finds that the $1/W(jw)$ locus will not change, but a lower M_1 means that the right hand end of the describing function plot will move toward the origin. Hence if M_1 is reduced too much the loci will not intersect. Evidently a compromise is again necessary to make $\delta(w)$ as small as possible, still ensuring an intersection of $1/W(jw)$ and the describing function. The

question here is whether, as M_1 is decreased, the end of the describing function moves in past the intersection point with the $1/W(jw)$ locus faster than the $\delta(w)$'s become small enough to enable the technique to work. If it does, a situation where the technique has failed cannot be corrected by decreasing M_1 alone.

The gain of $G_1(s)$ was left at 180, while M_1 was reduced from 0.5 to 0.4, and the method was applied. Again the method worked for the modified system. The results are also given in Table III.

TABLE III

GARBER - ROZENVASSER ESTIMATES FOR THE TWO MODIFIED SYSTEMS

Item	Possibility (1) system	Possibility (2) system
Gain of $G_1(s)$	130	180
M_1	0.5	0.4
Amplitude range	$1.51 \leq A \leq 2.09$	$1.78 \leq A \leq 2.48$
Frequency range	$3.16 \leq w \leq 3.42$	$3.11 \leq w \leq 3.44$
Describing function predictions	$A_b=1.77$ $w_b=3.32$	$A_b=2.06$ $w_b=3.32$
Bound on $\lvert x_h \rvert$	0.079 (use 0.08)	0.112 (use 0.11)
Bound on max $\lvert x \rvert$	2.17	2.59

Whereas in the original system condition (4.17) was satisfied down to and including w = 1.6, in the possibility (1) system it was satisfied down to and including w = 1.4, and in the possibility (2) system down to and including w = 1.5 (the $\varepsilon(w)$'s were calculated at increments of 0.1 rad./sec. in w). Also, in both cases a doubling back of the envelope was again noted as the circles increased in size.

Thus it is evident that in at least some cases where the Garber - Rozenvasser technique fails because one or both envelope intersections cannot be found, the method may be made to work by modifying either the linear or the nonlinear element appropriately. Due consideration must be given, however, to the maximum amount that these elements can be modified before the describing function and $1/W(jw)$ loci no longer intersect.

CHAPTER V

SHIFT OF GAIN INVESTIGATION

Now that the Garber - Rozenvasser technique had been made to work, a new item for investigation arose -- the possibility that, since $\delta(w)$ is proportional to the square of M_1, in a given system gain should be shifted from the nonlinearity to the linear element as much as possible to improve the estimates. It was thought that perhaps lowering M_1 and consequently raising the gain of the linear element to preserve the original loop gain would produce a net decrease in $\delta(w)$. If it did, then a "trade off" of gain would be possible as a method of improving the estimates.

The possibility was investigated for a modification of Rankine's original $G_1(s)$ - plus - saturation system, having $M_1 = 0.5$ and a linear element gain of 160. This system was chosen because in the light of earlier work it was fairly certain that the Garber - Rozenvasser technique would work for it. Two variations of this system were used in the investigation. In each case the loop gain was kept the same, and Rankine's value of $S = 3$ for the saturation nonlinearity was retained. Therefore, in each case the describing function predicts the same amplitude of oscillation. The cases chosen were:

Case (1) $M_1 = 0.5$, Gain = 160

Case (2) $M_1 = 0.4$, Gain = 200

Case (3) $M_1 = 0.3$, Gain = 800/3 = 266.67

The Garber - Rozenvasser method worked in each case, and estimates were calculated. The results are presented in Table IV.

TABLE IV

ESTIMATES FOR THREE CASES IN SHIFT OF GAIN INVESTIGATION

Item	Case (1)	Case (2)	Case (3)
Amplitude range	$2.01 \leq A \leq 3.11$	$2.02 \leq A \leq 3.14$	$2.02 \leq A \leq 3.11$
Frequency range	$3.02 \leq w \leq 3.47$	$3.02 \leq w \leq 3.47$	$3.02 \leq w \leq 3.47$
Describing function predictions	$A_b = 2.34$ $w_b = 3.32$	$A_b = 2.34$ $w_b = 3.32$	$A_b = 2.34$ $w_b = 3.32$
Bound on $\lvert x_h \rvert$	0.171 (use 0.17)	0.173 (use 0.17)	0.171 (use 0.17)
Bound on max $\lvert x \rvert$	3.28	3.31	3.28

For the system studied there appears to be no significant improvement in any of the estimates as a result of a shift of gain from the nonlinearity to the linear element. The procedure gives a net reduction in $\delta(w)$ (at $w = 3.0$ case (1) gives $\delta(w) = 0.036$, case (2) gives $\delta(w) = 0.029$, and case (3) gives $\delta(w) = 0.022$). However, raising the gain of the linear element causes the $1/W(jw)$ locus to move inward toward the origin (at $w = 3.0$, $1/W(jw)$ for cases (1), (2), and (3) is respectively $0.3000 - j\ 0.0375$, $0.2400 - j\ 0.0300$, and $0.1800 - j\ 0.0225$), which tends to offset the effect of the reduction in the $\delta(w)$'s.

In each case the numerical distance between the left and right hand envelope intersections decreases (in case (1) the distance is 0.423 - 0.296 = 0.127, while in case (2) it is 0.336 - 0.235 = 0.101 and in case (3) it is 0.252 - 0.178 = 0.074). But in each successive case the describing function locus is more compressed (in case (1) it extends from 0 to 0.5, in case (2) from 0 to 0.4, and in case (3) from 0 to 0.3). The net result is that the first harmonic amplitude ranges are essentially all the same.

One disadvantage of the system chosen for this investigation became apparent after the work had been done. The system chosen is rather close to Rankine's original $G_1(s)$ - plus - saturation system ($M_1 = 0.5$, Gain = 180), for which the technique failed because no left hand intersection could be found. The result is that in each case the left hand portion of the envelope crosses the describing function at a fairly small angle, and it is difficult to decide the exact numerical value of the intersection. Incidentally, this also gives rise to the fairly high value of A_h in each case. If a system for which the $1/W(jw)$ locus intersects the describing function almost vertically had been chosen, the numerical values of the left hand intersections could have been established with more certainty. This seems to be a rather minor criticism, and probably no significant improvement in the estimates would have been obtained had such a system been used in the investigation. Nevertheless it is worthy of mention.

Judging by the behaviour of the system investigated, a gain shift from the nonlinearity to the linear element in a given system does not seem a worthwhile method of improving the Garber - Rozenvasser estimates.

CHAPTER VI

APPLICATION OF THE GARBER - ROZENVASSER TECHNIQUE TO SOME HYPOTHETICAL CASES

At this point some consideration was given to several "border line" or "out-of-the-ordinary" cases. In the following discussion it is assumed that the nonlinearity involved is one, such as saturation, for which higher numerical values of the describing function correspond to smaller input amplitudes.

First, consider a low-gain oscillating system, that is one which has sufficient gain to exhibit a limit cycle but for which the $1/W(jw)$ locus crosses very close to the end of the describing function. For such a system there exists the possibility that when the Garber - Rozenvasser estimates are applied the right hand portion of the envelope will not intersect the describing function because the circles extend out too far. Rather it will lie beyond the end of the describing function. Even though such a system oscillates, an estimate of A_ℓ is not possible in the usual manner.

However, a little reflection reveals that an amplitude and a frequency range can still be obtained by recalling that the vector difference between the $1/W(jw)$ locus and the describing function must lie in a circle of radius $\delta(w)$. Hence the smallest possible first harmonic amplitude will be given by the end point of the describing function, and w_h will be that frequency for which the circle just touches the end point of the describing function. All the usual estimates can therefore be made for such a system.

As an illustration, the technique was applied to a modification of Rankine's original $G_1(s)$ - plus - saturation system, having a linear element gain of 123 and an M_1 of 0.5. The $1/W(jw)$ locus will pass through the end point of the describing function when the linear element gain is reduced to 120. At a gain of 123 the crossing occurs at 0.488 on the describing function, and the system should oscillate. The results obtained for the system are summarized in Table V. The right hand envelope crossing occurred at 0.525, but the describing function only extended to 0.5.

TABLE V

ESTIMATES FOR LOW-GAIN OSCILLATING SYSTEM

Amplitude range	$0 \leq A \leq 1.89$	(end point of describing function corresponds to amplitudes from 0 to 1.5)
Frequency range	$3.18 \leq w \leq 3.39$	
Describing function predictions	$A_b = 1.59$ $w_b = 3.32$	
Bound on $\lvert x_h \rvert$	0.065	(use 0.07)
Bound on max $\lvert x \rvert$	1.96	

Second, consider the complement of the first case, a system whose gain is not quite large enough to sustain an oscillation.[1] For this

[1] as determined by describing function estimates.

system the $1/W(jw)$ locus passes just beyond the end point of the describing function. Even though the system might not oscillate, if the gain is large enough the left hand portion of the envelope will still intersect the describing function, and just as in the first case an amplitude and a frequency range can still be found. In turn the other estimates can be made.

Although a bound can be put on the maximum magnitude of the response, it will in this case be a rather liberal one since the response will have zero amplitude. Nevertheless the bound is still meaningful. Also, the fact that the estimates give a frequency range, and not a zero frequency, is quite consistent, since the fact that the response has zero amplitude does not imply that it must also have zero frequency.

An example was not worked out to illustrate this case, since it seemed rather pointless to go to a lot of work simply to put a bound on a zero amplitude response. This "border line" case is mentioned here merely to show that the Garber - Rozenvasser estimates give valid results in a system where there is a "near miss" of the $1/W(jw)$ locus and the describing function.

The third and fourth cases are more ambiguous than the first two. Suppose that experimentally Rankine's original $G_1(s)$ - plus - saturation system does not oscillate when the linear element gain is set at, say, 117, while at a gain of 123 it does oscillate. Experimentally the gain may be increased starting at 117 until that critical gain for which the system just starts to oscillate is found. One of three cases can arise. Either (1) the oscillation can start at some

gain between 117 and 120, in which case there will be no intersection of the $1/W(jw)$ locus and the describing function; (2) it can start at a gain of 120; or (3) it can start between 120 and 123, including the value 123, in which cases there will be an intersection of the two loci. In the first instance the system would oscillate when the describing function predicts that it would not. In the second instance the system would start to oscillate at exactly that gain predicted by the describing function. In the third instance there would be some gain between 120 and that value which starts the oscillation where the system would not oscillate when the describing function predicts that it would. The first and third possibilities above, being cases where the describing function gives incorrect predictions, are considered further here as the third and fourth "border line" cases.

In the third "border line" case, then, the describing function predicts no oscillation. However, the Garber - Rozenvasser method will give all the usual estimates, this being a case of a "near miss" of the $1/W(jw)$ locus and the describing function. Then when the system is set up, it turns out that it oscillates. Evidently the Garber - Rozenvasser estimates have given useful information in a case where the describing function fails.

In the fourth "border line" case the describing function predicts an oscillation. The Garber - Rozenvasser technique again gives all the usual estimates. When set up, the system does not oscillate. The estimates have again given valid information (in the sense that zero amplitude will certainly be less than the bound placed on the amplitude

by the estimates) in a case where the describing function fails.

It was decided to simulate Rankine's original $G_1(s)$ - plus - saturation system on an analog computer and find the critical gain. One of possibilities (1), (2), and (3) would occur. If possibility (2) occurred, the system would not be investigated further, since the cases of interest were those where the describing function failed. If possibilities (1) or (3) (third or fourth "border line" cases) occurred, a typical system with a gain midway between the critical gain and 120 could be chosen. Then this system could be studied by applying the Garber - Rozenvasser method to it and by checking the estimates against the experimental amplitude and frequency of oscillation. Evidently, however, if the fourth "border line" case occurred, it would be rather futile to go through all the work involved in applying the estimates, simply to put a bound on a zero-amplitude response. Suffice it to say that in this case the estimates are meaningful but very liberal indeed. It was hoped that the third "border line" case would occur so that there would be a non-zero experimental amplitude with which to compare the estimated bound on the maximum magnitude of the response.

The experimental procedure followed and the results obtained are outlined in Chapter VII.

Thus it is seen that the Garber - Rozenvasser technique gives meaningful estimates in cases of a "near miss" or a "near hit" of the $1/W(jw)$ locus and the describing function. These are the cases where the describing function method, because of its approximate nature, is apt to yield erroneous predictions of system behaviour. The Garber -

Rozenvasser technique establishes definite bounds on the frequency and the maximum magnitude of the response. It would therefore seem that, because the behaviour of the system is not known a priori, in cases of a "near hit" or a "near miss" the Garber - Rozenvasser technique, even though it does not say whether or not the system will oscillate,[2] is superior to the describing function method in that it does not leave room for error.

---

[2]Graham and Hofmann, op. cit., Chapter III, consider the case of a "near miss" of the two loci. As noted before, they suggest as an explanation for the possible failure of the describing function method in this case that the higher harmonics of the response are critically important. They outline a "generalized periodic input describing function" technique for discovering whether or not a limit cycle will exist and if so determining its approximate amplitude and frequency. A disadvantage of the method, however, is that it requires a considerable amount of computation.

CHAPTER VII

EXPERIMENTAL RESULTS

Experimental results for comparison to estimated results

It was decided to obtain some experimental results for one or two of the systems for which the estimates had been calculated. The experimental results could be compared to the estimates to see how good the estimates actually are.

Rankine's original $G_1(s)$ - plus - saturation system was simulated on a PACE TR - 48 analog computer (Electronic Associates, Inc.), with provision being left for varying the gain of the linear element and M_1, the slope of the saturation characteristic. The details of the simulation are given in Appendix C.

Although reducing the gain on the linear element or on the nonlinear element is essentially the same procedure, it was decided to check both the possibility (1) and possibility (2) systems of Chapter IV, Section III since they are different and would therefore furnish two checks of the estimates. The system used in the shift of gain investigation was also studied experimentally since it would provide a third check of the estimates. All three cases (page 43) were tried experimentally, even though they all should have the same amplitude and frequency (being the same system), since the estimates had been worked out separately for each one. Finally, the first "border line" case of Chapter VI, for which the estimates appear on page 47, was tested.

These systems, it was felt, would give an indication of how accurate the Garber - Rozenvasser estimates are.

For each system in turn, the appropriate values of M_1 and linear element gain were set on the computer. An initial condition was applied to the response. The response was recorded on a Houston Instrument Corp. Model HR - 96 X-Y Recorder. The amplitude of the limit cycle was measured using a circuit explained in Appendix C, and the frequency was calculated from the recording.

The estimated results as well as the experimental results for each system are presented in Table VI on the next page.

TABLE VI

COMPARISON OF ESTIMATED AND EXPERIMENTAL RESULTS FOR SEVERAL SYSTEMS[1]

System	Linear element gain	M_1	DF amplitude prediction	G-R bound on max $\lvert x \rvert$	Experimental amplitude	DF frequency prediction (rad./sec.)	G-R frequency range (rad./sec.)	Experimental frequency (rad./sec.)
(a) reduced linear element gain	130	0.5	1.77	2.17	1.79	3.32	$3.16 \leq w \leq 3.42$	3.28
(b) reduced M_1	180	0.4	2.06	2.59	2.09	3.32	$3.11 \leq w \leq 3.44$	3.28
(c) shift of gain investigation, cases (1)	160	0.5	2.34	3.28	2.38	3.32	$3.02 \leq w \leq 3.47$	3.25
(2)	200	0.4	2.34	3.31	2.38	3.32	$3.02 \leq w \leq 3.47$	3.26
(3)	266.67	0.3	2.34	3.28	2.38	3.32	$3.02 \leq w \leq 3.47$	3.26
(d) first "border line" case	123	0.5	1.59	1.96	1.61	3.32	$3.18 \leq w \leq 3.39$	3.29

[1] DF denotes "describing function" and G-R denotes "Garber - Rozenvasser."

Table VII gives the percentages by which the various predicted quantities differ from the values obtained experimentally.

TABLE VII

PERCENTAGE DIFFERENCES BETWEEN PREDICTED AND EXPERIMENTAL VALUES[2]

System in Table VI	DF amplitude prediction from experimental amplitude	G-R bound on max |x| from experimental amplitude	DF frequency prediction from experimental frequency	G-R frequency predictions from experimental frequency	
				low bound	high bound
(a)	1.12% low	21.2% high	1.22% high	3.66% low	4.27% high
(b)	1.44% low	23.9% high	1.22% high	5.19% low	4.89% high
(c) (1)	1.68% low	37.8% high	2.16% high	7.08% low	6.77% high
(2)	1.68% low	39.0% high	1.84% high	7.36% low	6.45% high
(3)	1.68% low	37.8% high	1.84% high	7.36% low	6.45% high
(d)	1.24% low	21.7% high	0.91% high	3.34% low	3.04% high

[2]DF denotes "describing function" and G-R denotes "Garber - Rozenvasser."

In these cases, where the linear transfer function is of order three, the describing function is very accurate in predicting the amplitude of the response. On the other hand, the Garber - Rozenvasser bounds

on the maximum magnitude of the response are roughly 20% to 40% high. However, one important consideration is that the describing function underestimates the amplitude here, while the Garber - Rozenvasser bound overestimates it. In designing a system it might be harmful to underestimate the response. In such a case the Garber - Rozenvasser technique would be particularly useful in that the designer can be sure that the response will not exceed a certain value.

In the cases investigated the describing function predicts the frequency of oscillation accurately. Its prediction is high in all of them. In each case the experimental frequency falls within the range predicted by the Garber - Rozenvasser technique. The Garber - Rozenvasser frequency estimates are quite good in that the worst difference between a bound and an experimental frequency is 7.36%.

Critical gain determination

For the attempt to find the critical gain for the $G_1(s)$ - plus - saturation system, the linear element gain was initially set at 117. It was noted that no limit cycle is possible in the system if the amplitude falls below 1.5, at which the "knee" of the saturation characteristic occurs, since the system would then be linear and the oscillation would be damped. The response was recorded for several different initial conditions ranging from 1.0 to 6.0 until it became obvious whether or not the system exhibited a limit cycle. Since it did not, the gain was increased to 118 and the procedure repeated. The gain was increased by one each time until the critical value was found.

The system did not oscillate at a gain of 120, but did oscillate when the gain was increased to 121. However, the potentiometers on the TR - 48 could not be set to any more than three decimal places, so the exact value of the critical gain could not be found. It was known to be somewhere between 120 and 121 (or possibly at 121), but that was all. Nevertheless, it was evident that there would be some gain for which the system would not oscillate, even though the describing function predicted that it would. This corresponds to the fourth "border line" case in Chapter VI.

It had been hoped that the third "border line" case would occur, but it did not. As noted in Chapter VI there was no point in applying the Garber - Rozenvasser estimates in this case when it was known that the steady state response would have zero amplitude. Therefore, the investigation was not continued.

Experimental check of second Garber - Rozenvasser example

It was thought that in the light of the results of the first section of this chapter an analog computer check of Garber and Rozenvasser's second example would be worthwhile. Although Garber and Rozenvasser calculated all the estimates for the system, they gave no experimental results by way of comparison. Since in the previous experimental checks the Garber - Rozenvasser bounds on the maximum magnitude of the response were found to be 20% to 40% too high, it was thought that the authors' example should be studied to see if in their case the bound was any more accurate.

The system was simulated on the analog computer. The details of the simulation are given in Appendix C. When an initial condition was applied to the response, the system oscillated. The amplitude and frequency of the oscillation were measured as before, and results of 1.46 and 2.83 rad./sec. were obtained respectively.

Table VIII on the next page compares the authors' results for this example and the results obtained by the independent check carried out here and in Section II of Chapter IV. In each case the percentages by which the various predicted quantities differ from the appropriate experimental values, either the amplitude of 1.46 or the frequency of 2.83 rad./sec., are given.

The authors' bound on the maximum magnitude of the response is 46.5% too high. The check of the example gives a somewhat improved bound, but it is still 32.2% high. Therefore, it would seem that the 20% to 40% high bounds found for the systems investigated in the first section of this chapter are not unusually high. Rather, they are quite good compared to the results which Garber and Rozenvasser saw fit to publish.

TABLE VIII

COMPARISON OF ESTIMATES FROM ARTICLE AND

FROM CHECK TO EXPERIMENTAL RESULTS[3]

Item	Value quoted in article	Percentage difference from experimental value of quantity	Value obtained in check	Percentage difference from experimental value of quantity
DF amplitude prediction	1.55	6.16% high	1.45	0.685% low
G-R bound on max |x|	2.14	46.5% high	1.93	32.2% high
DF frequency prediction (rad./sec.)	2.82	0.354% low	2.83	no error
G-R frequency range (rad./sec.)	$2.75 \leq w \leq 2.90$	low bound 2.83% low high bound 2.48% high	$2.77 \leq w \leq 2.89$	low bound 2.12% low high bound 2.12% high

[3]DF denotes "describing function" and G-R denotes "Garber - Rozenvasser."

CHAPTER VIII

FURTHER COMMENTS ON THE GARBER - ROZENVASSER ESTIMATES

Investigation of "A - w diagrams"

The Garber - Rozenvasser estimates give a certain allowable range for A in the form $A_\ell \leq A \leq A_h$ and an allowable range for w in the form $w_\ell \leq w \leq w_h$. However, not all A, w pairs falling in these ranges are possible, since each w has a certain set of A values that can occur with it. It was decided to study the plotting of an "A - w diagram," which would show the various allowable values of A for each w in the range $w_\ell \leq w \leq w_h$.

First, consider the application of the Garber - Rozenvasser technique to the case where the $1/W(jw)$ locus and the describing function intersect at right angles as, say, in the authors' second example. Figure 8 shows the circles drawn at different w-values from w_ℓ to w_h to produce the envelope that defines the allowable range of A. It is seen from the diagram that at the frequency w_ℓ only the amplitude A_b (point A) is allowed, while at w_1 amplitudes in the range B - C of the describing function are possible. Finally, when the frequency reaches w_h, A_b is again the only value of A that can exist simultaneously (point H).

Figure 9 shows these results graphically in the form of an A - w diagram. The shaded region gives those A,w combinations that can

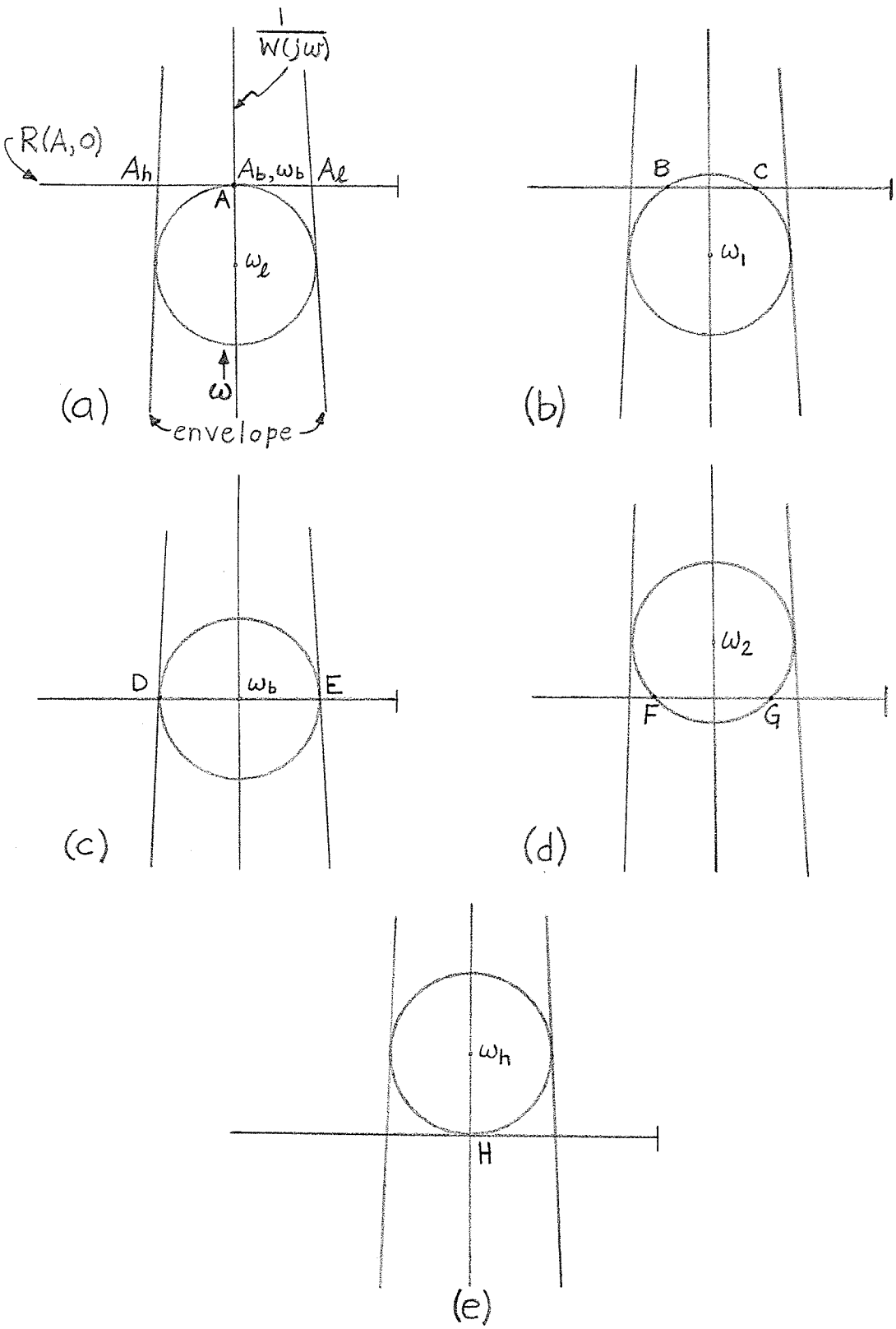

FIGURE 8

CIRCLES PRODUCING ESTIMATES FOR FIRST TYPE OF INTERSECTION

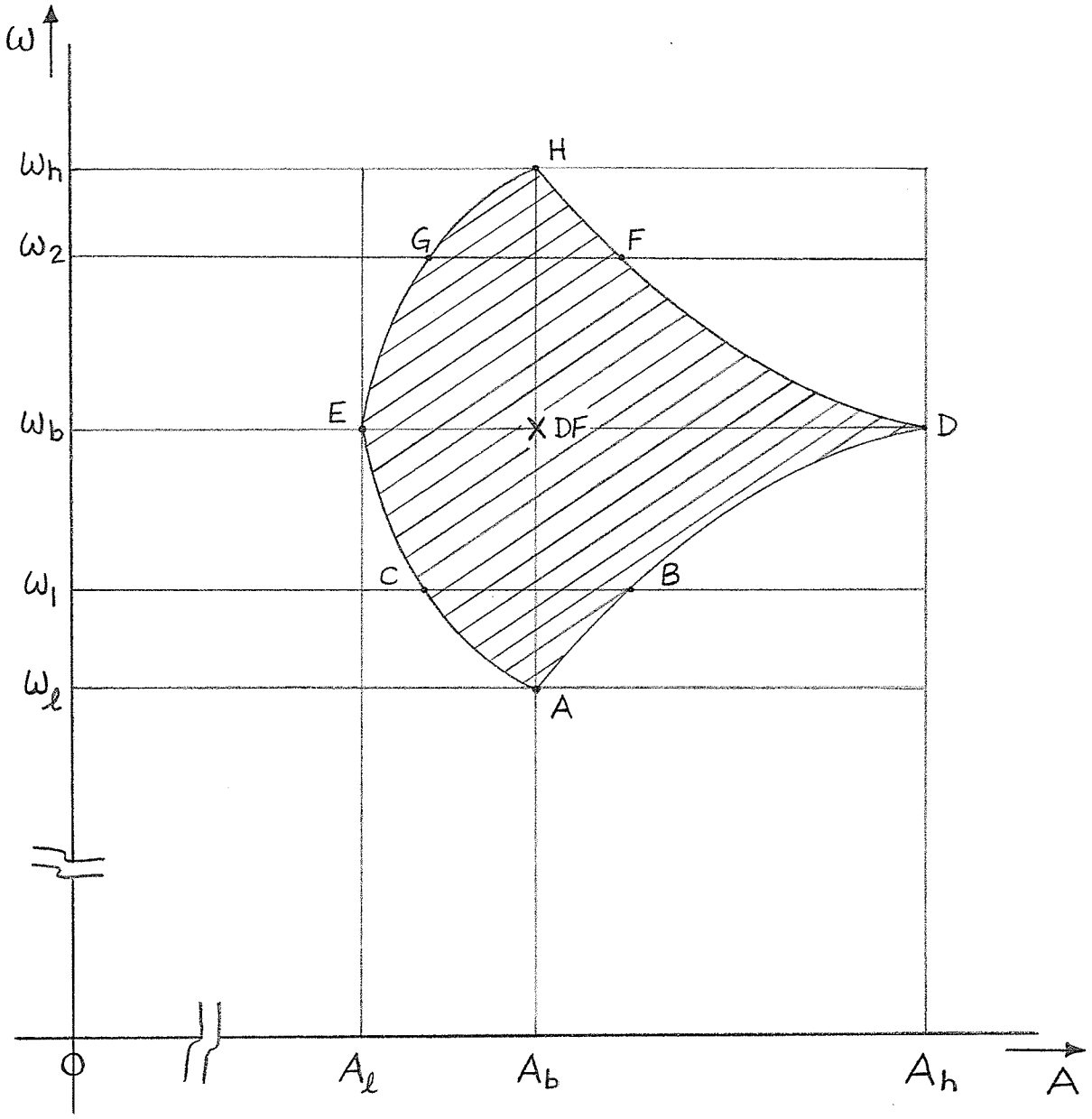

FIGURE 9

A - w DIAGRAM FOR FIRST TYPE
OF INTERSECTION

occur together. The point marked "DF" denotes the combination A_b, w_b predicted by the describing function method. Points on the diagram are lettered correspondingly to those in Figure 8. The diagram has been drawn assuming a saturation nonlinearity in the system. It is not drawn to scale, but rather is intended only to give a qualitative picture of the situation.

Several observations can be made regarding Figure 9. A saturation nonlinearity has been assumed. Because of the form of its describing function, A_b will not lie midway between A_ℓ and A_h but will be closer to A_ℓ. However, one cannot tell where w_b will fall with respect to w_ℓ and w_h, since the $\delta(w)$'s become smaller as w increases, but successive points on the $1/W(jw)$ locus may become farther apart or closer together as w increases. If the successive points become closer together, as in the authors' second example, then the effect of the decrease in $\delta(w)$ will be somewhat neutralized and w_b will lie approximately half way between w_ℓ and w_h. If, however, the successive points on $1/W(jw)$ become farther apart, as was the case in those modifications of Rankine's original $G_1(s)$ - plus - saturation system studied previously, the effects will complement each other, with the result that w_b will lie closer to w_h than to w_ℓ. This effect will be small because the $\delta(w)$'s will not decrease very much over the small range of w considered, and successive points on $1/W(jw)$ will not become very much farther apart. The shapes of segments of the diagram can be obtained qualitatively by considering the form of the saturation describing function.[1] For instance, the shape of segment A - B -

---

[1]Gibson, op. cit., Figure 9.15 on page 367.

D arises from the fact that as one moves from point A toward lower numerical values of the describing function, the amplitude increases moderately at first, then more rapidly. Similarly, for A - C - E as one moves from point A toward higher numerical values of the describing function, the amplitude decreases moderately at first, then more slowly. The shapes of segments D - F - H and E - G - H can be justified by a similar argument.

The foregoing procedure was repeated for the case where the $1/W(jw)$ locus intersects the describing function at an angle, assuming that both the right hand and left hand envelope intersections are available. This was the case, for example, for the possibility (1) and possibility (2) systems investigated in Section III of Chapter IV. Figure 10 shows the circles for different w-values from w_ℓ to w_h. Figure 11 is the A - w diagram for this case, again assuming a saturation nonlinearity.

The right and left hand envelope intersections will be approximately the same numerical distance from the intersection of the $1/W(jw)$ locus and the describing function. Hence A_b will again lie closer to A_ℓ than to A_h. As before, if successive points on the $1/W(jw)$ locus become closer together as w increases, then w_b will lie about half way between w_ℓ and w_h, but if successive points become farther apart, w_b will lie closer to w_h than to w_ℓ. In those examples studied previously which apply to this case, successive points on $1/W(jw)$ became farther apart as w increased, so that w_b should lie slightly closer to w_h than to w_ℓ. Segments A - B and I - K - L of Figure 11

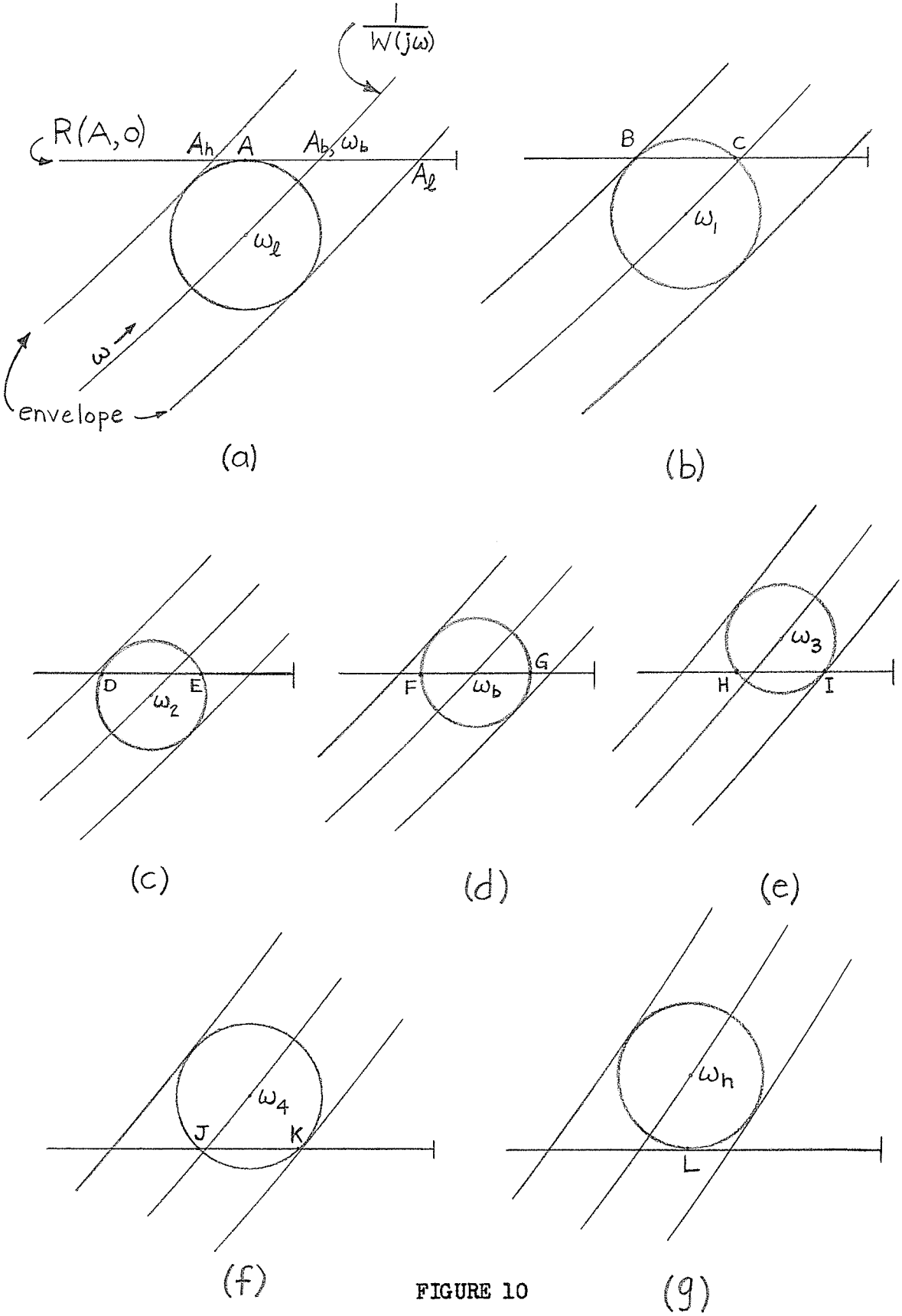

FIGURE 10

CIRCLES PRODUCING ESTIMATES FOR SECOND TYPE OF INTERSECTION

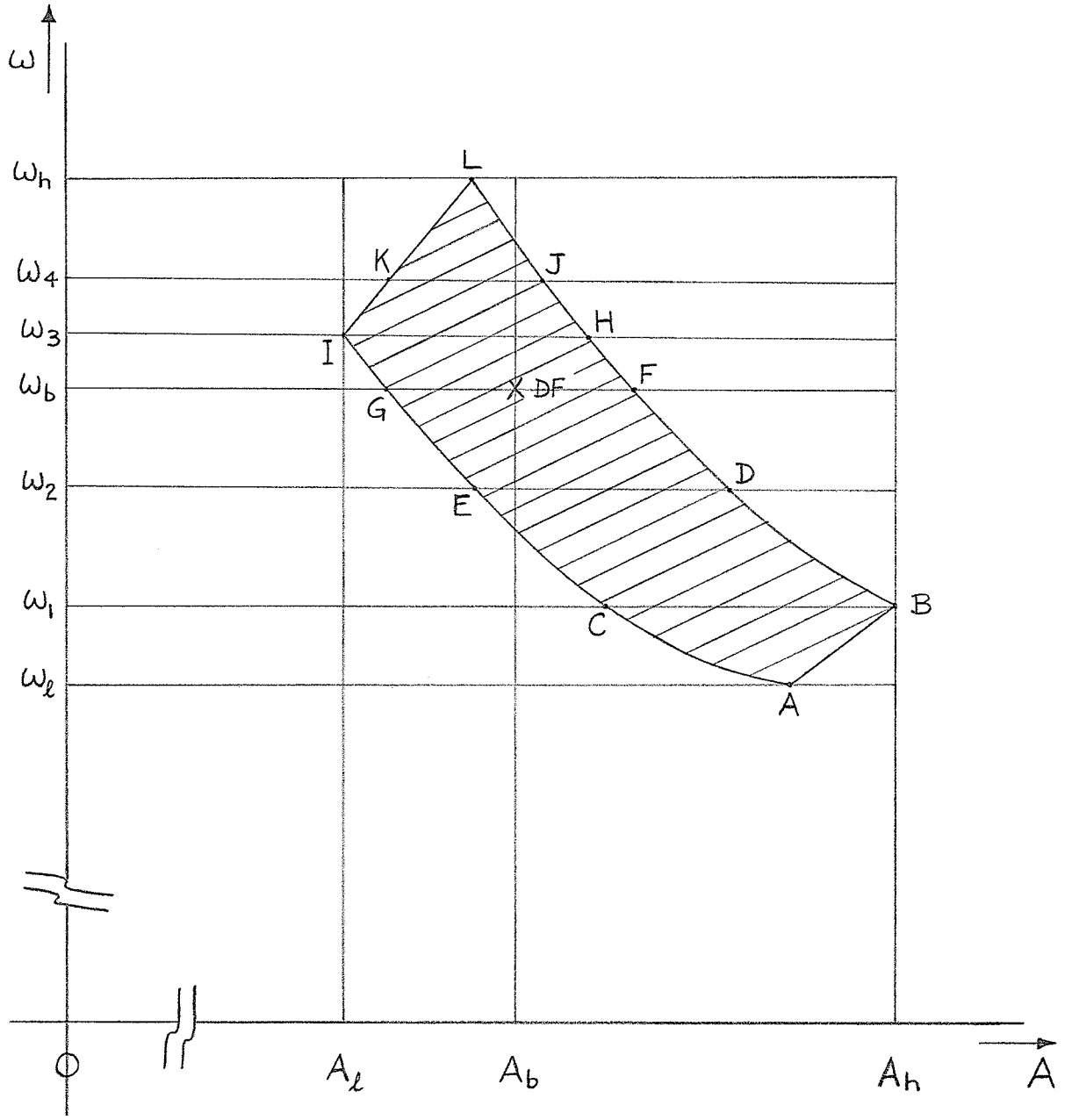

FIGURE 11

A - w DIAGRAM FOR SECOND TYPE
OF INTERSECTION

are approximately linear because they correspond to a very small range of the describing function. The shapes of segments B - D - F - H - J - L and A - C - E - G - I are given by the same reasoning as used in the previous case.

Finally, the case where the 1/W(jw) locus intersects the describing function at an angle, but only the left hand envelope intersection is available, was investigated. An example of this situation is the first "border line" case of Chapter VI. Figure 12 shows the circles for different w-values from w_ℓ to w_h, while Figure 13 is the A - w diagram for this case, assuming a saturation nonlinearity.

The end point of the describing function corresponds to a range of input amplitudes from zero to the value at which the "knee" of the saturation characteristic occurs. Thus points E and H in Figure 13 appear on the A - w diagram, not as a single amplitude, but as a range of amplitudes. "A"$_{\text{end of DF}}$ represents the amplitude at the "knee" of the saturation. In this case A_b will lie close to $A_{\text{end of DF}}$ because the 1/W(jw) intersection will be close to the end of the describing function. By the same argument as used in the previous case, w_b should lie closer to w_h than to w_ℓ. The effect could even be more pronounced here because in the previous case the w_h circle only had to touch the describing function at its lowest point, while here the circle will probably have to touch the end point of the describing function before hitting its lowest point (see Figure 14, page 70). Segment A - B of Figure 13 is approximately linear because it corresponds to a very small range of the describing function. The shapes of

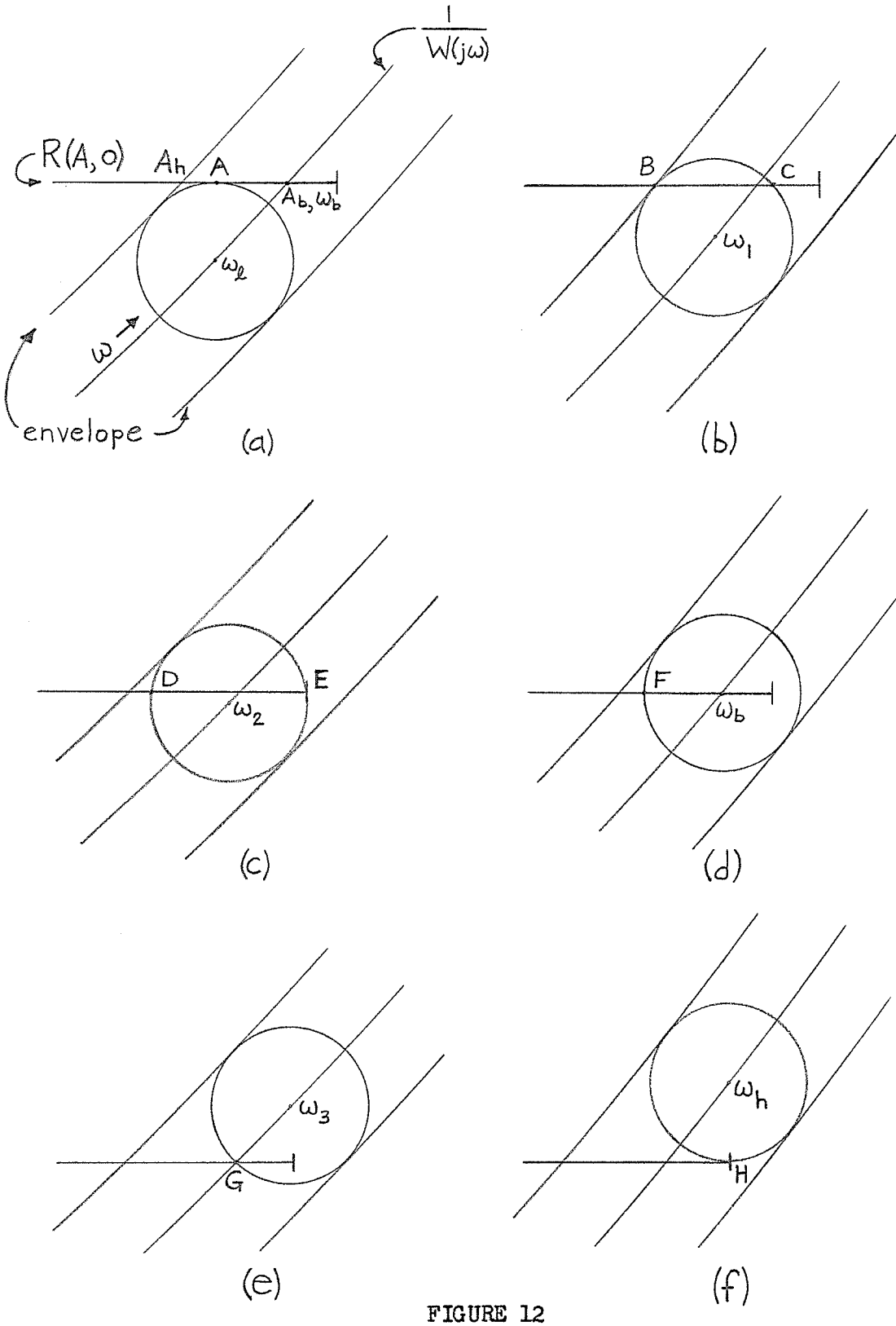

FIGURE 12

CIRCLES PRODUCING ESTIMATES FOR THIRD TYPE OF INTERSECTION

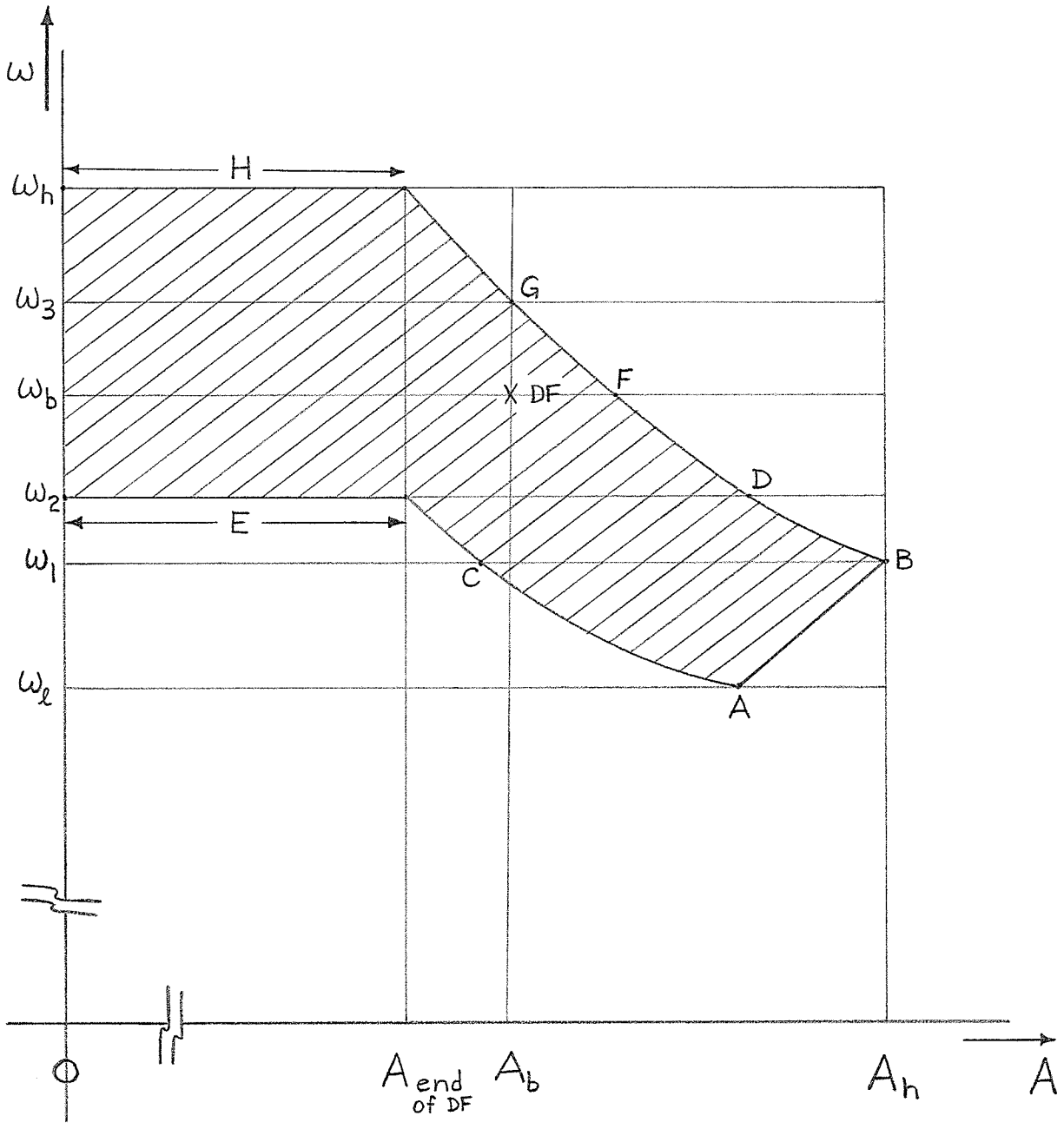

FIGURE 13

A - w DIAGRAM FOR THIRD TYPE OF INTERSECTION

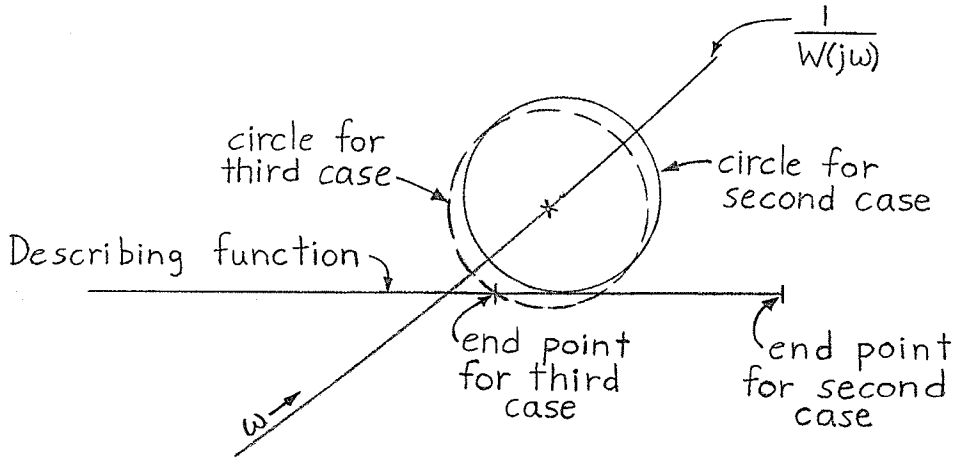

FIGURE 14

w_h CIRCLES FOR SECOND AND THIRD TYPES OF INTERSECTION

segments A - C - E and B - D - F - G - H are given by the same reasoning as used in the first case, but the curvature is less since a smaller range of the describing function is covered by the envelope here.

The observations made above are verified by the various systems for which the Garber - Rozenvasser estimates have been found. For the first case, in the authors' second example (using the results obtained in the check, Section II of Chapter IV, rather than those quoted by the authors) A_b (1.45) is closer to A_ℓ (1.19) than to A_h (1.76), and w_b (2.83) lies half way between w_ℓ (2.77) and w_h (2.89). For the second case, in the possibility (1) system of Chapter IV, Section III A_b (1.77) is closer to A_ℓ (1.51) than to A_h (2.09), while w_b (3.32) is closer to w_h (3.42) than to w_ℓ (3.15). Similarly, in the possibility (2) system of Chapter IV, Section III A_b (2.06) is closer to A_ℓ (1.78) than to A_h (2.48), and w_b (3.32) is closer to w_h (3.44) than to w_ℓ (3.11). For the third case, in the first "border line" system of Chapter VI A_b (1.59) is close to $A_{\text{end of DF}}$ (1.50), A_h being 1.89, and w_b (3.32) is closer to w_h (3.39) than to w_ℓ (3.18).

Attempts to improve the estimates

Inequality (5.10) of Garber and Rozenvasser's article gives the bound on $|x_h(t)|$ as

$$|x_h(t)| \leq M_1 A_h \max_{w_\ell \leq w \leq w_h} \frac{w\mathcal{E}^*(w)}{1 - M_1\epsilon(w)}$$

It was shown in Chapter III that an equivalent statement of the bound is

$$|x_h(t)| \leq \frac{\pi A_h}{4M_1} \delta(w_\ell) \qquad \text{(III - 3)}$$

The bound involves A_h and w_ℓ. However, from the previous discussion on A - w diagrams it is evident that an amplitude of A_h and a frequency of w_ℓ cannot occur together. The point (A_h, w_ℓ) does not fall in the allowable shaded regions of Figures 9, 11, and 13. It appears that the authors, in going from the basic relation, inequality (4.18), to inequality (5.10) have computed the right hand side of inequality (4.18) at the point (A_h, w_ℓ) simply because its value at that point is larger than its value at any point inside the shaded region.

Consider inequality (4.18). For a given value of w the bound on Δ is linear in A, or in other words

$$\Delta \leq \text{(constant)}.\ A \qquad \text{(VIII - 1)}$$

where the constant is given by

$$\text{constant} = \frac{\pi}{4M_1}\ \delta(w) \qquad \text{(VIII - 2)}$$

The constant, being proportional to $\delta(w)$, will increase as w decreases. Now for each w, A has a maximum allowable value. Therefore, it would seem logical to take each allowable value of w, $w_\ell \leq w \leq w_h$, compute $\pi/4M_1 \cdot \delta(w)$ for it, $\delta(w)$ being already known, use for A the maximum allowable A for that w, and calculate the bound on Δ. This would give a bound on Δ for each value of w. Then the maximum of all these bounds would be selected as the bound on Δ over the whole allowable range of w. By this method a tighter bound on Δ than that given by Garber and Rozenvasser could be found, which would in turn give a tighter bound on the maximum magnitude of the response.

Some observations can be made about the above procedure. For each w the bound on Δ will occur along the right hand (maximum ampli-

tude) boundary of the A - w diagram, and hence the bound on Δ over the whole shaded region will occur on this boundary as well. For example, in Figure 11 on page 66 the bound on Δ over the whole shaded region occurs somewhere along the boundary L - J - H - F - D - B - A. Furthermore, still with reference to Figure 11, the highest value of the bound on Δ for all $w_l \leq w \leq w_h$ will occur at w_l (point B) because $\delta(w)$ and the maximum allowable value of A are largest there for this range of w. Hence the bound on Δ need only be calculated for w-values in the range $w_\ell \leq w \leq w_l$ to find the bound over the whole shaded region.

Since the bound on Δ is a function of A and w, it can be plotted in three-dimensional form over the shaded region of the A - w diagram. Another way to plot the bound, which is easier to visualize, is to plot it against A for fixed values of w. Figure 15 is a qualitative sketch of the bound on Δ against A for various w-values from w_h down to w_ℓ, for the A - w diagram Figure 11. A-values in Figure 15 are lettered correspondingly to those in Figure 11.

The procedure for finding a tighter bound on $|x_h|$ than that given by Garber and Rozenvasser is recapitulated below. First, the bound on Δ is calculated at w_l, where A attains its maximum value, A_h. It is given by

$$\text{Bound at } w_l = \frac{\pi}{4M_l}\,\delta(w_l) \cdot A_h \qquad \text{(VIII - 3)}$$

This bound is larger than that for any w from w_h to w_l. Next, the bound is calculated at w-values between w_l and w_ℓ, and at w_ℓ. Then the

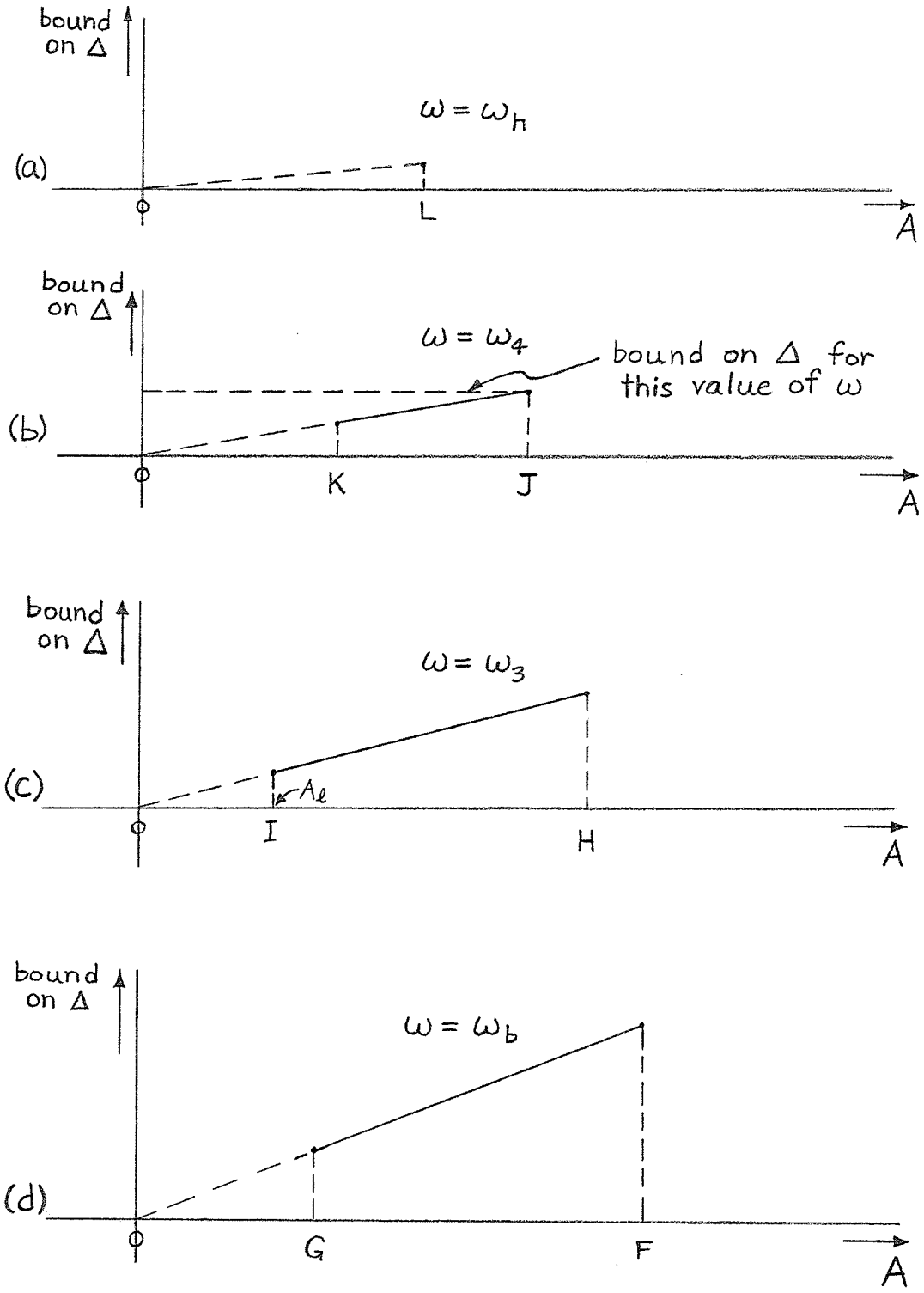

FIGURE 15

SKETCH OF BOUND ON Δ AGAINST A AT VARIOUS w-VALUES FOR FIGURE 11

continued...

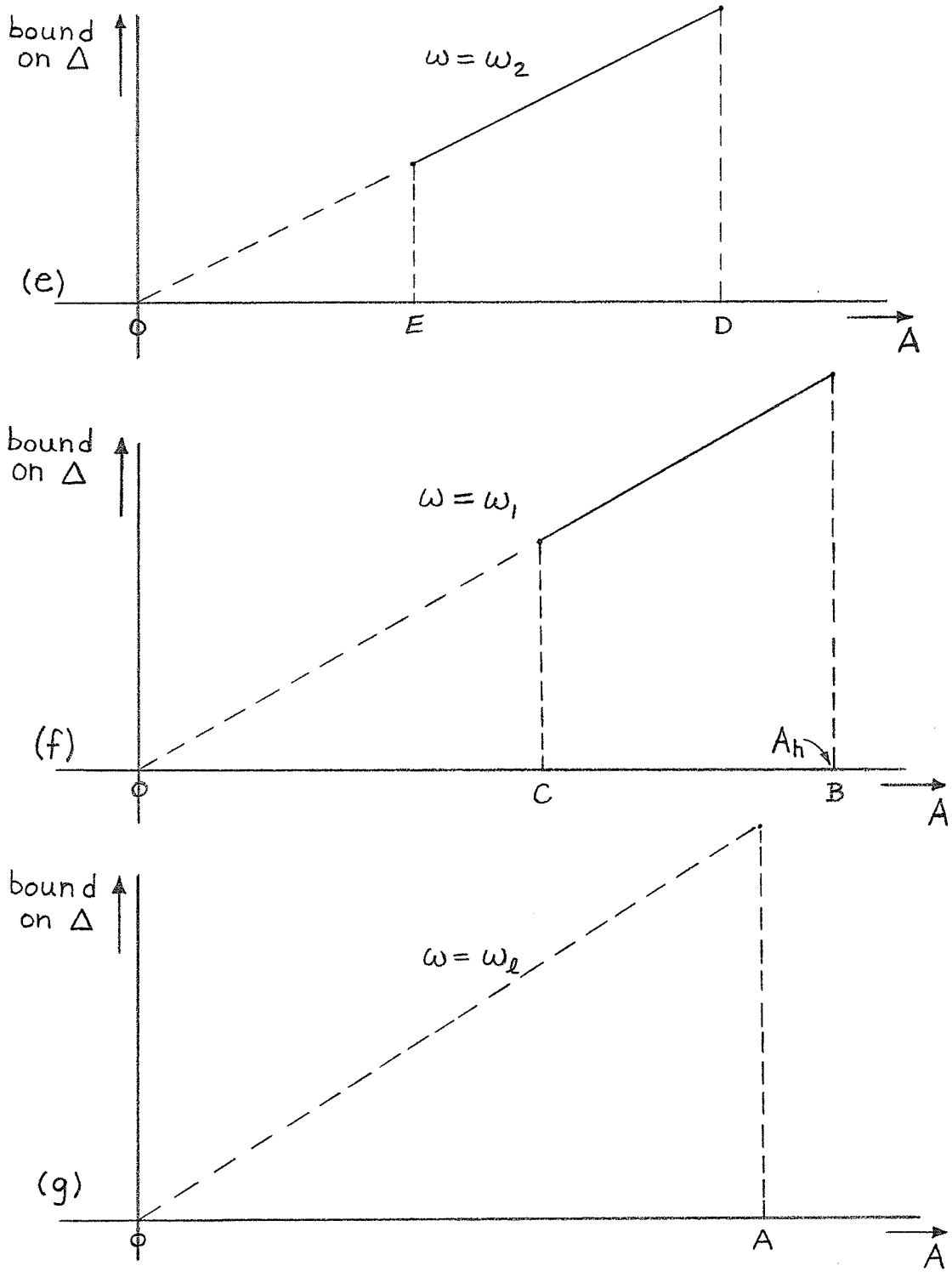

FIGURE 15 (cont'd.)

SKETCH OF BOUND ON Δ AGAINST A AT VARIOUS w-VALUES FOR FIGURE 11

largest of these bounds is taken as the bound on $|x_h|$ and is used in the calculation of the bound on the maximum magnitude of the response.

Therefore, the information that is required for an attempt to improve the authors' bound on $|x_h|$ includes the frequency w_1 at which A achieves its maximum value A_h, frequencies and their maximum amplitudes between w_1 and w_ℓ, and the one value of A possible at w_ℓ, A_h and w_ℓ being already known. In cases where the $1/W(jw)$ locus intersects the describing function at an angle, w_1 will be close to w_ℓ (Figures 11 and 13), so the attempt to improve the estimate should not involve too much calculation.

It was decided to apply the foregoing procedure to one of the example systems studied. Although the three cases of the shift of gain investigation produced the worst estimates, one was not selected for this study. It was evident that the liberality of these estimates was due mainly to the largeness of A_h, resulting from the fact that the cases chosen were close to the critical case having no left hand envelope intersection, and not to a large bound on $|x_h|$. Rather, the possibility (2) system of Chapter IV, Section III, having $M_1 = 0.4$ and a linear element gain of 180, was selected.

The values $A_h = 2.48$ and $w_\ell = 3.11$ have already been obtained for this system (see Table III, page 41). The frequency at which A_h occurred was found to be $w_1 = 3.14$. Table IX presents the maximum allowable amplitude A_{max}, $\delta(w)$, and the bound on $|x_h|$, calculated to three decimal places, for $w_\ell \leq w \leq w_1$. The bound on $|x_h|$ is found in

each case from

$$\text{Bound on } |x_h| = \frac{\pi}{4M_1} A_{max} \cdot \delta(w)$$

$$= \frac{\pi}{1.6} A_{max} \cdot \delta(w) \qquad \text{(VIII - 4)}$$

TABLE IX

DATA FOR ATTEMPTED IMPROVEMENT OF BOUND ON $|x_h|$

w (rad./sec.)	A_{max}	$\delta(w)$	Bound on $\lvert x_h \rvert$
w_ℓ = 3.11	2.46	0.023	0.111
3.12	2.47	0.022	0.107
3.13	2.47	0.022	0.107
w_1 = 3.14	2.48 = A_h	0.022	0.107

The bound obtained using A_h and w_ℓ was 0.112.

The procedure for improving the bound on $|x_h|$ involves a fair amount of work after all. For each w-value of interest, the point on the $1/W(jw)$ locus must be located, $\delta(w)$ must be found, the circle of radius $\delta(w)$ must be drawn and its appropriate intersection with the describing function found so that A_{max} can be calculated, and finally the bound on $|x_h|$ must be found. The "improved" bound on $|x_h|$ for the example is 0.111, which occurs at w_ℓ. The calculation of the bound on the maximum magnitude of the response, however, can only be carried out to an accuracy of two decimal places, this being all the accuracy with which A-values can be obtained from Rankine's describing function plot. Therefore, in either case a value of 0.11 would be used as the bound

on $|x_h|$ in the final calculation, so that as far as the bound on the maximum magnitude of the response is concerned nothing has been accomplished.

In cases where the $1/W(jw)$ locus intersects the describing function at an angle, the value of A at w_ℓ will be very close to A_h (2.46 and 2.48 respectively in the example above). Also, because w_1 is close to w_ℓ and the frequency range $w_\ell \leq w \leq w_h$ is usually high enough that $\delta(w)$ does not vary too rapidly over it, $\delta(w_1)$ will be close to $\delta(w_\ell)$ (0.022 and 0.023 in the example above). Therefore, the bound on $|x_h|$ calculated anywhere between w_1 and w_ℓ, which gives the bound over the whole allowable A - w region, will be almost the same as that calculated using A_h and w_ℓ. When A_h and w_ℓ are used, then, one calculation gives a bound which is for all practical purposes as good as any "improved" bound obtainable by the method outlined, which involves a lot more work. Note that in this example an attempt was made to reduce a quantity which comprises 4.25% of the total bound on the maximum magnitude of the response. Even if an improvement of almost 50% in the bound on $|x_h|$, say from 0.11 to 0.06, resulted, the bound on the maximum magnitude of the response would only be reduced from 2.59 (23.9% high) to 2.54 (21.5% high), an improvement which certainly does not seem to justify the work put into it.

The bound on $|x_h|$ proposed by Garber and Rozenvasser is sufficiently accurate in cases where the $1/W(jw)$ locus intersects the describing function at an angle and the filtering of the linear element

is fairly good, that is where the effect of higher harmonics is relatively small to begin with. For example, in none of the six cases in Table VI does the bound on $|x_h|$ make up more than 5.2% of the bound on the maximum magnitude of the response. In such cases an attempt to improve the bound on $|x_h|$ is not practical from an engineering standpoint, in that it yields a small return for a large amount of tedious work.

Possibly it might be more fruitful to try to improve the bound on $|x_h|$ in cases where the $1/W(jw)$ locus intersects the describing function at right angles and the filtering is poor. Then the w-value (w_b in this case) at which A achieves the value A_h would be substantially larger than w_ℓ, the value of A at w_ℓ and $\delta(w_b)$ would be substantially smaller than A_h and $\delta(w_\ell)$ respectively, and the bound on $|x_h|$ would make up a larger portion of the bound on the maximum magnitude of the response.

From the foregoing example it is evident that, at least in cases where the $1/W(jw)$ locus intersects the describing function at an angle and the filtering is reasonably good, the amount by which the bounds on the maximum magnitude of the response are too liberal is an inherent fault of the Garber - Rozenvasser method, not the result of putting too liberal a bound on $|x_h|$ for the sake of computational convenience.

CHAPTER IX

CONCLUSIONS AND RECOMMENDATIONS FOR FUTURE WORK

The scope of the investigation is considerably narrower than originally intended (Chapter I, Section II). Although the problem originally included both the autonomous and non-autonomous cases, the study was of necessity restricted to the autonomous case and for reasons outlined on page 18 to the combined Garber - Rozenvasser article.

It has been seen that for some systems the Garber - Rozenvasser technique may fail in that it does not give one or both of the required intersections of the envelope and the describing function plot. However, in some of these cases the technique can be made to work by modifying either the linear or the nonlinear element appropriately, with certain reservations. Also, the possibility of a doubling back of the envelope to give a second pair of intersections was noted and discussed. Garber and Rozenvasser's second example system was checked and several discrepancies were noted. Their amplitude and frequency ranges seemed to be tighter than they should be, while their bounds on $|x_h|$ and max $|x|$ seemed too liberal. A doubling back of the envelope was also noted in their example.

The possibility of improving the estimates for a given system by means of a shift of gain from the nonlinearity to the linear element was investigated. However, the shift of gain produced no significant improvement in any of the estimates for the system studied.

The application of the Garber - Rozenvasser technique to some hypothetical "border line" cases was considered. The technique, it was seen, will give meaningful estimates in cases of a "near miss" or a "near hit" of the $1/W(jw)$ locus and the describing function, the cases where the describing function method may fail altogether.

Experimental results were obtained for several systems as a check on the estimates. It was found that the describing function method predicted the amplitude of the response accurately, but underestimated it. The Garber - Rozenvasser bounds on the maximum magnitude of the response were, on the other hand, 20% to 40% too high. Also, the describing function method predicted the frequency accurately, but overestimated it. In every case the Garber - Rozenvasser frequency range enclosed the experimental frequency. An attempt was made to investigate a system for which the Garber - Rozenvasser technique gave valid results when the describing function method failed. The case of interest, however, did not arise, so the work was not pursued.

An experimental check of Garber and Rozenvasser's second example was carried out because no experimental results were given in their article. Their quoted bound on the maximum magnitude of the response was found to be 46.5% high. In the light of this result, previously obtained bounds 20% to 40% high did not seem quite so bad.

Finally, the plotting of "A - w diagrams" showing the allowable values of A for each w in the range $w_\ell \leq w \leq w_h$ was studied for three different types of intersection of the $1/W(jw)$ locus and the describing function. The observations made during the drawing of the diagrams were

verified by systems for which the estimates had been found. Garber and Rozenvasser's bound on $|x_h(t)|$, it was noted, is computed at a point not allowed by the A - w diagrams. An attempt was made to improve the bound on $|x_h(t)|$, but after an example had been worked out it was seen that at best the technique would yield a small improvement for a large amount of work. At least in cases where the $1/W(jw)$ locus intersects the describing function at an angle and the filtering is fairly good, it was concluded that the Garber - Rozenvasser bound on $|x_h(t)|$ is sufficiently accurate for engineering purposes. It became apparent that the liberality of the bounds on the maximum magnitude of the response was not due to too liberal a bound on $|x_h(t)|$, but rather was an inherent fault of the method.

Some comments can be made about the two methods used for calculating the parameters $\mathcal{E}(w)$ and $\mathcal{E}^*(w)$ -- the approximate, or series, method of inequalities (4.19) and (4.20) as outlined in Chapter III, and the exact method of inequalities (A - 1) and (A - 4) as outlined in Appendix A. For a system involving a high-order linear transfer function $W(p)$, the exact calculation of $\mathcal{E}(w)$ and $\mathcal{E}^*(w)$ is difficult if the denominator polynomial has complex roots because the sum over the roots involves the calculation of several terms. On the other hand, in this case the series for $\mathcal{E}(w)$ and $\mathcal{E}^*(w)$ converge rapidly, so that the approximate method gives an accurate estimation of the two parameters. For a system involving a low-order $W(p)$, the series for $\mathcal{E}(w)$ and $\mathcal{E}^*(w)$ do not converge as rapidly, but the exact calculation is considerably easier

since fewer terms are involved in the sum over the roots. Therefore, the two methods of calculation complement each other, and one or the other can be used depending on the particular form of W(p).

Truxal[1] states that from an engineering viewpoint a "complete evaluation of the describing-function analysis" should answer, for instance, the question, "Under what conditions might the describing-function analysis indicate stability, while the actual system is unstable?" The Garber - Rozenvasser technique provides a partial answer to this question. With reference to the systems investigated, if the $1/W(jw)$ locus misses the describing function but a left hand envelope intersection is still available (i.e. a "near miss" of the two loci), then the describing function method indicates stability, while the Garber - Rozenvasser method indicates the possibility of instability. The Garber - Rozenvasser method does not say that a limit cycle will exist; it says that one might exist. Under these conditions, then, the describing function method could indicate stability when in fact the system is unstable. The engineer, says Truxal, would prefer a "quantitative criterion" that would answer the question above. The Garber - Rozenvasser technique provides such a criterion.

Several recommendations for future work can be made on the basis of this study. With regard to the attempts made in Chapter IV, Section III to modify a system so that the Garber - Rozenvasser technique would

---

[1] Truxal, op. cit., p. 611.

work for it, perhaps other modifications to the linear transfer function than simply changing its gain could be tried. For instance, possibly the poles and/or zeros of the transfer function could be altered to produce a more desirable $1/W(jw)$ locus, that is, one with a lower "dip" and a steeper intersection with the describing function. Also, it would be worthwhile to apply the shift of gain procedure outlined in Chapter V to a system for which the $1/W(jw)$ locus intersects the describing function vertically or almost vertically. In this case the left hand envelope intersections could be found more accurately, and perhaps more conclusive statements could be made about the procedure. Finally, further attention should be given to the possibility of improving Garber and Rozenvasser's bound on $|x_h|$ by the method detailed under the second heading of Chapter VIII. This attention should be concentrated on systems for which the $1/W(jw)$ locus intersects the describing function at right angles and the filtering of the linear element is poor.

BIBLIOGRAPHY

(1) Bass, R. W., "Mathematical Legitimacy of Equivalent Linearization by Describing Functions," Proceedings of the First International Congress of the International Federation of Automatic Control (I. F. A. C.), Moscow, 1960. London: Butterworths, 1961. pp. 895-905.

(2) Garber, E. D., "Error Estimation in the Describing Function Method," Automation and Remote Control, Vol. 24, 1963, pp. 449-458.

(3) Garber, E. D., and E. N. Rozenvasser, "The Investigation of Periodic Regimes of Nonlinear Systems on the Basis of the Filter Hypothesis," Automation and Remote Control, Vol. 26, 1965, pp. 274-285.

(4) Gibson, John E., Nonlinear Automatic Control. New York: McGraw-Hill Book Company, Inc., 1963. 585 pp.

(5) Gille, J-C, M. J. Pélegrin, and P. Decaulne, Feedback Control Systems. New York: McGraw-Hill Book Company, Inc., 1959. 793 pp.

(6) Glatenok, I. V., "On the Foundation of the Harmonic Balance Method," Symposium on Nonlinear Vibrations, Kiev, U.S.S.R., September, 1961.

(7) Graham, Dunstan, and Lee Gregor Hofmann, "Investigations of Describing Function Technique." Technical Report AFFDL - TR - 65 - 137, Air Force Flight Dynamics Laboratory, Research and Technology Division, Air Force Systems Command, Wright-Patterson Air Force Base, Ohio, February, 1966.

(8) Graham, Dunstan, and Duane McRuer, Analysis of Nonlinear Control Systems. New York: John Wiley and Sons, Inc., 1961. 482 pp.

(9) Hale, Jack K., Oscillations in Nonlinear Systems. New York: McGraw-Hill Book Company, Inc., 1963. 180 pp.

(10) Johnson, E. C., "Sinusoidal Analysis of Feedback-Control Systems Containing Nonlinear Elements," Trans. AIEE, Vol. 71, Part II. Applications and Industry, July, 1952, pp. 169-181.

(11) Kazarinoff, Nicholas D., Analytic Inequalities. New York: Holt, Rinehart and Winston, 1961. 89pp.

(12) Kislyakov, V. S., "Foundations for the Application of the Harmonic Linearization Method to an Investigation of Periodic Oscillations in Systems with Lag," Automation and Remote Control, Vol. 21, 1960, pp. 1051-1056.

(13) Quazza, G., "On the Validity of the Describing Function -, Tsypkin - and Hamel - Methods for the Study of Self Oscillations in On - Off Systems," Alta Frequenza, Vol. XXXII, No. 2, February, 1963, pp. 142-156.

(14) Rankine, Robert R., Jr., "An Evaluation of Selected Describing Functions of Control System Nonlinearities." Report GGC/EE/64-16, Air Force Institute of Technology, Air University, United States Air Force, Wright-Patterson Air Force Base, Ohio, 1964. 130 pp.

(15) Rozenvasser, E. N., "On the Accurate Determination of Periodic Regimes in Sectionally Linear Automatic Control Systems," Automation and Remote Control, Vol. 21, 1960, pp. 902-910.

(16) Sandberg, I. W., "On the Response of Nonlinear Control Systems to Periodic Input Signals," The Bell System Technical Journal, Vol. XLIII, No. 3, May, 1964, pp. 911-926.

(17) Truxal, John G., Automatic Feedback Control System Synthesis. New York: McGraw-Hill Book Company, Inc., 1955. 675 pp.

APPENDIX A

EXACT CALCULATION OF $\varepsilon(w)$ AND $\varepsilon^*(w)$

For the quantity

$$\bar{I}(w) = \sqrt{2 \sum_{s=0}^{\infty} \left| W[(2s+1)iw] \right|^2}$$

in inequality (2.11), Garber and Rozenvasser derive the closed form (2.13)

$$\bar{I}(w) = \sqrt{\frac{\pi}{w} \sum_{\rho=1}^{n} \frac{K(\lambda_\rho)\ K(-\lambda_\rho)}{D'(\lambda_\rho)\ D(-\lambda_\rho)} \tanh \left(\frac{-\pi\ \lambda_\rho}{2w}\right)}$$

$\lambda_\rho (\rho = 1, 2, \ldots n)$ being the roots of the equation $D(\lambda) = 0$.[1] Hence, when j is used in place of i in the complex notation,

$$\sqrt{2\left|W(jw)\right|^2 + 2 \sum_{s=1}^{\infty} \left| W[(2s+1)jw] \right|^2} = \sqrt{\frac{\pi}{w} \sum_{\rho=1}^{n} \frac{K(\lambda_\rho)\ K(-\lambda_\rho)}{D'(\lambda_\rho)\ D(-\lambda_\rho)} \tanh \left(\frac{-\pi\lambda_\rho}{2w}\right)}$$

from which

$$\sqrt{2 \sum_{s=1}^{\infty} \left| W[(2s+1)jw] \right|^2} = \sqrt{\frac{\pi}{w} \sum_{\rho=1}^{n} \frac{K(\lambda_\rho)\ K(-\lambda_\rho)}{D'(\lambda_\rho)\ D(-\lambda_\rho)} \tanh \left(\frac{-\pi\lambda_\rho}{2w}\right) - 2\left|W(jw)\right|^2}$$

Therefore, the following inequality can be written in place of inequality (4.19):

$$\varepsilon(w) \leq \sqrt{\frac{\pi}{w} \sum_{\rho=1}^{n} \frac{K(\lambda_\rho)\ K(-\lambda_\rho)}{D'(\lambda_\rho)\ D(-\lambda_\rho)} \tanh \left(\frac{-\pi\lambda_\rho}{2w}\right) - 2\left|W(jw)\right|^2} \qquad (A - 1)$$

---

[1] Garber and Rozenvasser, op. cit., pp. 277-278.

A similar closed form can be derived for the bound on $\mathcal{E}^*(w)$ given by inequality (4.20). Let

$$W_1(p) = \frac{W(p)}{p} = \frac{K(p)}{pD(p)} \qquad (A - 2)$$

Then

$$\left|W_1[(2s+1)jw]\right|^2 = \frac{\left|W[(2s+1)jw]\right|^2}{(2s+1)^2\, w^2}$$

If $W_1(p)$ is defined as

$$W_1(p) = \frac{K_1(p)}{D_1(p)} \qquad (A - 3)$$

the procedure used above yields, when applied to this new transfer function

$$\sqrt{2\sum_{s=1}^{\infty}\left|W_1[(2s+1)jw]\right|^2} = \sqrt{\frac{\pi}{w}\sum_{\rho=1}^{n}\frac{K_1(\lambda_\rho)\,K_1(-\lambda_\rho)}{D_1'(\lambda_\rho)\,D_1(-\lambda_\rho)}\tanh\left(\frac{-\pi\lambda_\rho}{2w}\right) - 2\left|W_1(jw)\right|^2}$$

where the sum is now taken over the roots of the equation $D_1(\lambda) = 0$. Hence

$$\sqrt{2\sum_{s=1}^{\infty}\frac{\left|W[(2s+1)jw]\right|^2}{(2s+1)^2\, w^2}} = \sqrt{\frac{\pi}{w}\sum_{\rho=1}^{n}\frac{K_1(\lambda_\rho)\,K_1(-\lambda_\rho)}{D_1'(\lambda_\rho)\,D_1(-\lambda_\rho)}\tanh\left(\frac{-\pi\lambda_\rho}{2w}\right) - 2\left|W_1(jw)\right|^2}$$

from which the following inequality can be written in place of inequality (4.20):

$$\mathcal{E}^*(w) \leq \sqrt{\frac{\pi}{w}\sum_{\rho=1}^{n}\frac{K_1(\lambda_\rho)\,K_1(-\lambda_\rho)}{D_1'(\lambda_\rho)\,D_1(-\lambda_\rho)}\tanh\left(\frac{-\pi\lambda_\rho}{2w}\right) - 2\left|W_1(jw)\right|^2} \qquad (A - 4)$$

Inequalities (A - 1) and (A - 4) can now be used to obtain exact rather than approximate bounds on $\mathcal{E}(w)$ and $\mathcal{E}^*(w)$, and in turn exact values of $\delta(w)$ can be found.

For the second Garber - Rozenvasser example,

$$W(p) = \frac{p}{p^2 + 0.8p + 8}$$

from which

$$K(p) = p$$

$$D(p) = p^2 + 0.8p + 8$$

$$D'(p) = 2p + 0.8$$

The roots of $D(\lambda) = 0$ are

$$\left.\begin{aligned} \lambda_1 &= -0.4 + j\,2.80 \\ \lambda_2 &= -0.4 - j\,2.80 \end{aligned}\right\} \qquad (A - 5)$$

In inequality (A - 1) the coefficient of the first term in the sum is

$$\frac{K(\lambda_1)\,K(-\lambda_1)}{D'(\lambda_1)\,D(-\lambda_1)} = \frac{\lambda_1\,(-\lambda_1)}{(2\lambda_1 + 0.8)\,(\lambda_1^2 - 0.8\lambda_1 + 8)}$$

When the numerical value of λ_1 is used, the first coefficient becomes

$$\text{Coefficient of first term in (A - 1) sum} = \frac{7.6800 + j\,2.2400}{25.0880 + j\,3.5840} \qquad (A - 6)$$

Similarly, the second coefficient in the sum is

$$\text{Coefficient of second term in (A - 1) sum} = \frac{7.6800 - j\,2.2400}{25.0880 - j\,3.5840} \qquad (A - 7)$$

The second coefficient is the complex conjugate of the first.

It can be shown from the exponential definition of tanh z that for a complex number $z = a + j\,b$,

$$\tanh(z^*) = (\tanh z)^* \qquad (A - 8)$$

where the star denotes the complex conjugate. Also, the following equation may be derived for tanh z:

$$\tanh z = \frac{(e^{2a} - e^{-2a}) + j\,4 \sin b \cos b}{\cos^2 b(e^a + e^{-a})^2 + \sin^2 b(e^a - e^{-a})^2} \qquad (A - 9)$$

Hence for $z^* = a - j\,b$,

$$\tanh(z^*) = \frac{(e^{2a} - e^{-2a}) - j\,4\sin b\cos b}{\cos^2 b(e^a + e^{-a})^2 + \sin^2 b(e^a - e^{-a})^2} \qquad (A - 10)$$

Rationalization of the first coefficient in the (A - 1) sum, given by equation (A - 6), yields

Coefficient of first term in (A - 1) sum

$$= \frac{200.70400}{642.25280} + j\,\frac{28.67200}{642.25280} \qquad (A - 11)$$

Hence

Coefficient of second term in (A - 1) sum

$$= \frac{200.70400}{642.25280} - j\,\frac{28.67200}{642.25280} \qquad (A - 12)$$

In the (A - 1) sum, if the first term involves the factor $\tanh(z)$ the second term will involve the factor $\tanh(z^*)$, since the roots λ_1 and λ_2 are complex conjugates. The first term in the sum will have the form

$$\underbrace{(c + j\,d)}_{\substack{\text{first}\\ \text{coefficient}}}\ \underbrace{(e + j\,f)}_{\substack{\text{first}\\ \tanh\\ \text{factor}}} = (ce - df) + j\,(cf + de)$$

The second term in the sum will have the form

$$\underbrace{(c - j\,d)}_{\substack{\text{second}\\ \text{coefficient}}}\ \underbrace{(e - j\,f)}_{\substack{\text{second}\\ \tanh\\ \text{factor}}} = (ce - df) - j\,(cf + de)$$

Therefore, the sum in inequality (A - 1) will have the form

$$\text{Sum in (A - 1)} = 2(ce - df) \qquad (A - 13)$$

where the factors, identified from equations (A - 11) and (A - 9), are:

$$c = \frac{200.70400}{642.25280} \qquad (A - 14)$$

$$d = \frac{28.67200}{642.25280} \qquad (A - 15)$$

$$e = \frac{(e^{2a} - e^{-2a})}{\cos^2 b(e^a + e^{-a})^2 + \sin^2 b(e^a - e^{-a})^2} \qquad (A - 16)$$

$$f = \frac{4 \sin b \cos b}{\cos^2 b(e^a + e^{-a})^2 + \sin^2 b(e^a - e^{-a})^2} \qquad (A - 17)$$

The writing of tanh z as e + j f from (A - 9) assumes the form z = a + j b. The parameters a and b must now be identified. The quantity z has been identified as the argument of the tanh factor in the first term of the sum, so that

$$z = \frac{-\pi\lambda_1}{2w} = \frac{-\pi}{2w}(-0.4 + j\,2.80) = \frac{0.2\pi}{w} + j\left(\frac{-1.40\pi}{w}\right)$$

Thus

$$a = \frac{0.2\pi}{w} \qquad (A - 18)$$

$$b = \frac{-1.40\pi}{w} \qquad (A - 19)$$

These two parameters are used in the evaluation of e and f.

Now, for the transfer function W(p) given,

$$W(jw) = \frac{j\,w}{(8 - w^2) + j\,0.8w}$$

so that

$$2|W(jw)|^2 = \frac{2w^2}{(8 - w^2)^2 + 0.64w^2} \qquad (A - 20)$$

Finally, the use of (A - 13) and (A - 20) in inequality (A - 1) yields the result

$$\varepsilon(w) \leq \sqrt{\frac{2\pi}{w}(ce - df) - \frac{2w^2}{(8-w^2)^2 + 0.64w^2}} \qquad (A - 21)$$

where c, d, e, and f are given by (A - 14) to (A - 17) respectively.

In inequality (A - 4) for $\varepsilon^*(w)$ the following transfer function is used (equation (A - 2)):

$$W_1(p) = \frac{W(p)}{p} = \frac{1}{p^2 + 0.8p + 8} \qquad (A - 22)$$

Hence from equation (A - 3),

$$K_1(p) = 1$$

$$D_1(p) = p^2 + 0.8p + 8$$

$$D_1'(p) = 2p + 0.8$$

The roots of the equation $D_1(\lambda) = 0$ are

$$\left.\begin{aligned} \lambda_1 &= -0.4 + j\,2.80 \\ \lambda_2 &= -0.4 - j\,2.80 \end{aligned}\right\} \qquad (A - 23)$$

In inequality (A - 4) the coefficient of the first term in the sum is

$$\frac{K_1(\lambda_1)\,K_1(-\lambda_1)}{D_1'(\lambda_1)\,D_1(-\lambda_1)} = \frac{1}{(2\lambda_1 + 0.8)(\lambda_1^2 - 0.8\lambda_1 + 8)}$$

When the numerical value of λ_1 is used, the first coefficient becomes

$$\text{Coefficient of first term in (A - 4) sum} = \frac{1}{25.0880 + j\,3.5840}$$

$$= \text{(when rationalized)} \quad \frac{25.08800}{642.25280} - j\,\frac{3.58400}{642.25280} \qquad (A - 24)$$

Similarly, the second coefficient in the sum is

$$\text{Coefficient of second term in (A - 4) sum}$$

$$= \frac{25.08800}{642.25280} + j\,\frac{3.58400}{642.25280} \qquad (A - 25)$$

Since the roots of $D_1(\lambda) = 0$ are exactly the same as those of $D(\lambda) = 0$, the tanh factors in each of the two terms in the (A - 4) sum will have the same form as in the previous development for $\varepsilon(w)$. The first term in the sum will have the form

$$\underbrace{(m - j\,n)}_{\substack{\text{first}\\ \text{coefficient}}} \quad \underbrace{(e + j\,f)}_{\substack{\text{first}\\ \text{tanh}\\ \text{factor}}} = (me + nf) + j\,(mf - ne)$$

The second term will have the form

$$\underbrace{(m + j\,n)}_{\substack{\text{second}\\ \text{coefficient}}} \quad \underbrace{(e - j\,f)}_{\substack{\text{second}\\ \text{tanh}\\ \text{factor}}} = (me + nf) - j\,(mf - ne)$$

Therefore, the sum in inequality (A - 4) will have the form

$$\text{Sum in (A - 4)} = 2(me + nf) \qquad \text{(A - 26)}$$

where m and n, identified from equation (A - 24), are:

$$m = \frac{25.08800}{642.25280} \qquad \text{(A - 27)}$$

$$n = \frac{3.58400}{642.25280} \qquad \text{(A - 28)}$$

and e and f are given as before by equations (A - 16) and (A - 17) respectively, in which a and b are given by (A - 18) and (A - 19).

For the transfer function $W_1(p)$,

$$W_1(jw) = \frac{1}{(8-w^2) + j\,0.8w}$$

so that

$$2\left|W_1(jw)\right|^2 = \frac{2}{(8-w^2)^2 + 0.64w^2} \qquad \text{(A - 29)}$$

Finally, the substitution of (A - 26) and (A - 29) into inequality (A - 4) gives

$$\varepsilon^{*}(w) \leq \sqrt{\frac{2\pi}{w}(me + nf) - \frac{2}{(8-w^2)^2 + 0.64w^2}} \qquad (A - 30)$$

where e, f, m, and n are given respectively by equations (A - 16), (A - 17), (A - 27), and (A - 28).

The exact bounds on $\varepsilon(w)$ and $\varepsilon^{*}(w)$ may be calculated from inequalities (A - 21) and (A - 30). For a given value of w, a and b are calculated, then e and f are determined. Next, $\varepsilon(w)$ can be found, condition (4.17) checked, and, if it holds, $\varepsilon^{*}(w)$ calculated. Finally, the exact value of $\delta(w)$ can be found.

As noted in Section II of Chapter IV, the exact values of $\delta(w)$ were computed for the w-values to be plotted in the check of Garber and Rozenvasser's second example, and were compared to the values obtained from the series calculation of $\varepsilon(w)$ and $\varepsilon^{*}(w)$. Table X on the next page compares the two sets of $\delta(w)$ values for those frequencies used in the plotting. The $\delta(w)$ values are given to three decimal places although in this particular case, because of the nature and orientation of the $1/W(jw)$ and describing function loci, they were only plotted to two decimal places. For the $\delta(w)$'s obtained by series estimation of $\varepsilon(w)$ and $\varepsilon^{*}(w)$, the number of terms required in the series to obtain the specified accuracy is also given.

As seen from Table X the two $\delta(w)$ values differ at only three frequencies, 1.4, 3.1, and 4.0. In each instance they differ only in the third decimal place, so that the plotting is not affected.

TABLE X

COMPARISON OF APPROXIMATE AND EXACT $\delta(w)$ VALUES

w(rad./sec.)	$\delta(w)$ from series estimation of $\varepsilon(w)$ and $\varepsilon^*(w)$	Number of terms required in series	Exact $\delta(w)$
1.3	1.70	2102	1.70
1.4	0.849	2290	0.850
1.5	0.570	2437	0.570
1.6	0.431	2553	0.431
1.7	0.348	2646	0.348
1.8	0.292	2722	0.292
1.9	0.253	2785	0.253
2.0	0.223	2837	0.223
2.1	0.200	2881	0.200
2.2	0.181	2919	0.181
2.3	0.165	2951	0.165
2.4	0.153	2979	0.153
2.5	0.142	3004	0.142
2.6	0.132	3025	0.132
2.7	0.124	3044	0.124
2.8	0.117	3061	0.117
2.9	0.110	3076	0.110
3.0	0.105	3088	0.105
3.1	0.100	3100	0.099
3.2	0.095	3111	0.095
3.3	0.091	3121	0.091
3.4	0.087	3130	0.087
3.5	0.083	3139	0.083
3.6	0.080	3146	0.080
3.7	0.077	3153	0.077
3.8	0.074	3159	0.074
3.9	0.072	3165	0.072
4.0	0.070	3171	0.069

APPENDIX B

EXAMPLE CALCULATION OF GARBER-ROZENVASSER ESTIMATES

The calculation of the estimates is given in detail for the possibility (1) system of Chapter IV, Section III. This is Rankine's original $G_1(s)$-plus-saturation system with the linear element gain reduced from 180 to 130.

Following the procedure outlined in Chapter III, one writes

$$W(s) = -G(s) = \frac{-130}{(s+1)(s+2)(s+3)} = \frac{-130}{s^3+6s^2+11s+6}$$

Hence

$$W(jw) = \frac{-130}{(6-6w^2) + j\, w(11-w^2)}$$

$$\frac{1}{W(jw)} = \frac{6(w^2-1)}{130} + j\,\frac{w(w^2-11)}{130} \qquad (B-1)$$

The second and third columns of Table XI on page 100 give the real and imaginary parts of equation (B - 1) evaluated at the w-values of interest.

Now for the calculation of $\varepsilon(w)$ and $\varepsilon^*(w)$,

$$W(jkw) = \frac{130}{6(k^2w^2-1) + j\, kw(k^2w^2-11)}$$

so that

$$2|W(jkw)|^2 = \frac{3.38 \times 10^4}{36(k^2w^2-1)^2 + k^2w^2(11-k^2w^2)^2} \qquad (B-2)$$

The use of (B - 2) in inequalities (4.19) and (4.20) respectively yields

$$\varepsilon(w) \leq \sqrt{\sum_{k=3,5,7,\ldots}^{\infty} \left[\frac{3.38 \times 10^4}{36(k^2w^2-1)^2 + k^2w^2(11-k^2w^2)^2} \right]} \qquad (B - 3)$$

$$\varepsilon^*(w) \leq \sqrt{\sum_{k=3,5,7,\ldots}^{\infty} \left[\frac{3.38 \times 10^4}{k^2w^2\{36(k^2w^2-1)^2 + k^2w^2(11-k^2w^2)^2\}} \right]} \qquad (B - 4)$$

The results of the $\delta(w)$ calculations from inequalities (B - 3) and (B - 4) and the calculation procedure outlined in Chapter III are given in the extreme right hand column of Table XI. The number of terms required in the $\varepsilon(w)$ series to attain the specified accuracy is also given.

The calculations are all given to three decimal places since that is the maximum accuracy with which the values can be plotted. Figure 16 is a graph of $\delta(w)$ against w.

Figure 17 is the plot for this system from the data of Table XI. The 1/W(jw) and R(A,o) loci are marked. The R(A,o) locus extends out to 0.5 since that is the slope of the saturation characteristic.

The circles from w = 4.0 down to w = 2.3 give two intersections of the envelope and the describing function, as desired. As w goes lower, the circles rapidly increase in size, and the envelope doubles back. The circles for w = 1.5 and w = 1.4 are too large to plot.

The intersections occur at 0.412 and 0.498 on the describing function. From curve 4 on page 38 of Rankine's thesis, with K = 0.5 and S = 3 for the saturation nonlinearity, the amplitude values corres-

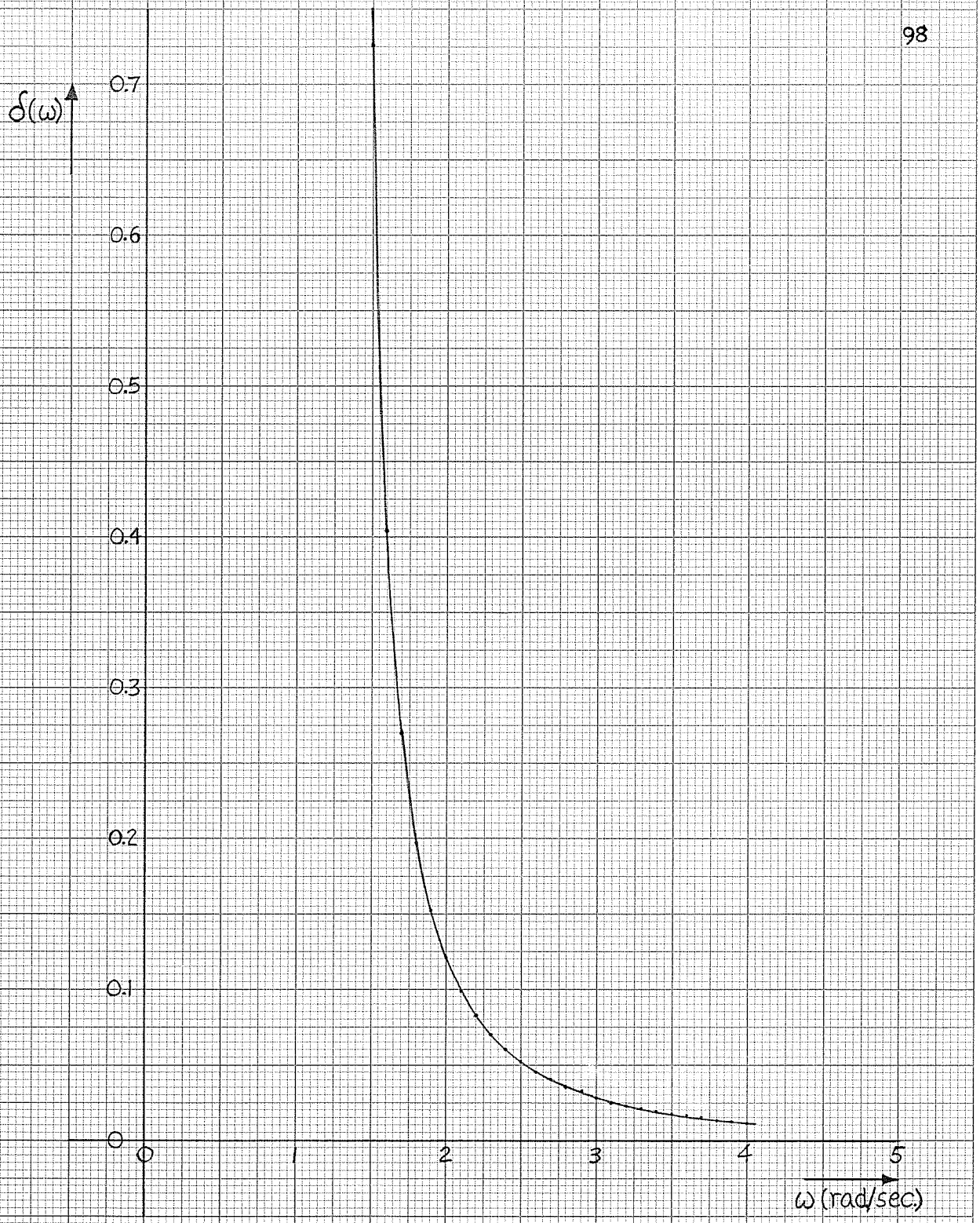

FIGURE 16

PLOT OF δ(w) AGAINST w FOR EXAMPLE CALCULATION OF ESTIMATES

H. W. Duncan
Dec./66

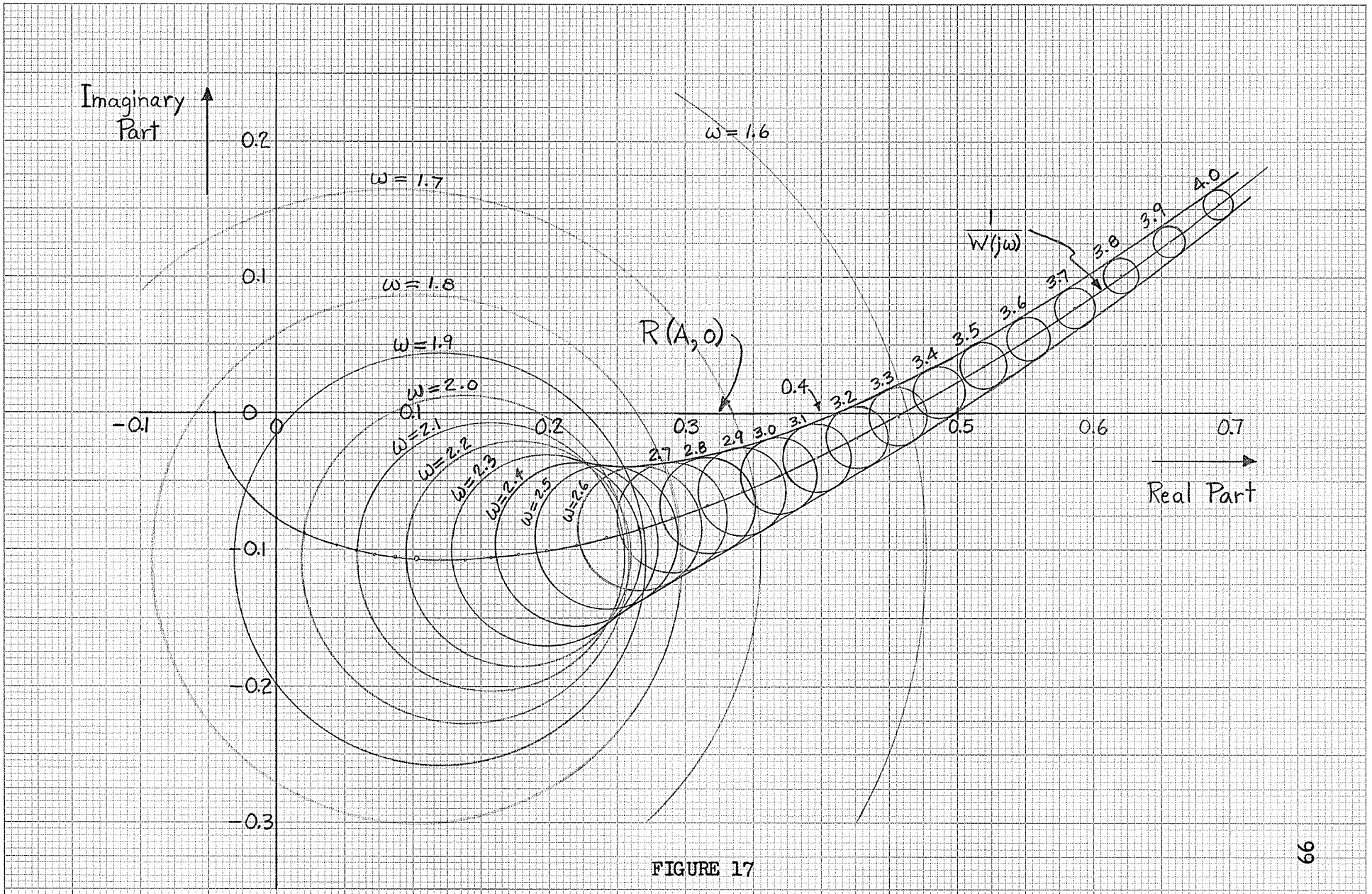

FIGURE 17

GARBER-ROZENVASSER DIAGRAM FOR EXAMPLE CALCULATION OF ESTIMATES

G. W. Duncan
Dec./66

TABLE XI

DATA FOR EXAMPLE CALCULATION OF ESTIMATES

w (rad./sec.)	Real part of 1/W(jw)	Imaginary part of 1/W(jw)	No. of terms in $\mathcal{E}(w)$ series	$\delta(w)$
0.0	-0.046	0.000		
0.1	-0.046	-0.008		
0.2	-0.044	-0.017		
0.3	-0.042	-0.025		
0.4	-0.039	-0.033	39 [1]	cond.(4.17)violated
0.5	-0.035	-0.041	35	cond.(4.17)violated
0.6	-0.030	-0.049	32	cond.(4.17)violated
0.7	-0.024	-0.057	30	cond.(4.17)violated
0.8	-0.017	-0.064	28	cond.(4.17)violated
0.9	-0.009	-0.071	27	cond.(4.17)violated
1.0	0.000	-0.077	26	cond.(4.17)violated
1.1	0.010	-0.083	26	cond.(4.17)violated
1.2	0.020	-0.088	25	cond.(4.17)violated
1.3	0.032	-0.093	25	cond.(4.17)violated
1.4	0.044	-0.097	24	2.489
1.5	0.058	-0.101	24	0.726
1.6	0.072	-0.104	24	0.404
1.7	0.087	-0.106	24	0.270
1.8	0.103	-0.107	23	0.197
1.9	0.120	-0.108	23	0.152
2.0	0.138	-0.108	23	0.121
2.1	0.157	-0.106	23	0.099
2.2	0.177	-0.104	23	0.083
2.3	0.198	-0.101	23	0.070
2.4	0.220	-0.097	23	0.060
2.5	0.242	-0.091	23	0.052
2.6	0.266	-0.085	23	0.045
2.7	0.290	-0.077	23	0.040
2.8	0.316	-0.068	22	0.035
2.9	0.342	-0.058	22	0.032
3.0	0.369	-0.046	22	0.028
3.1	0.397	-0.033	22	0.025
3.2	0.426	-0.019	22	0.023
3.3	0.456	-0.003	22	0.021
3.4	0.487	0.015	22	0.019
3.5	0.519	0.034	22	0.017
3.6	0.552	0.054	22	0.016
3.7	0.586	0.077	22	0.015
3.8	0.620	0.101	22	0.013
3.9	0.656	0.126	22	0.012
4.0	0.692	0.154	22	0.011

[1] As noted on page 28, $\mathcal{E}(w)$ was only calculated for w-values from 0.4 on.

ponding to these two points are found to be 2.085 and 1.515 respectively. Therefore, the amplitude range is

$$1.51 \leq A \leq 2.09 \qquad (B - 5)$$

The frequency range extends between the centres of circles tangent to the describing function. From Figure 17, w_ℓ evidently lies between 3.1 and 3.2 rad./sec. A linear interpolation procedure is used between these two frequencies to estimate w_ℓ.

At w = 3.1 and w = 3.2 the imaginary parts of $1/W(jw)$ are - 0.033 and - 0.019 respectively, while the $\delta(w)$ values are 0.025 and 0.023 respectively. The frequency is increased from 3.1 rad./sec. in steps of 0.01 rad./sec., with a linear increase in the imaginary part of $1/W(jw)$ over a small range of w and a similar linear decrease in $\delta(w)$ assumed, until a frequency is reached at which the imaginary part of $1/W(jw)$ and $\delta(w)$ are numerically equal. This frequency is w_ℓ. A similar procedure is used to estimate w_h.

Although it is evident from Table XI that the increase in the imaginary part value between two successive frequencies does not remain constant as w goes from zero to 3.7 rad./sec., this is nevertheless a good approximation over a frequency range of the order of 0.1 rad./sec. Also, the assumption of a linear decrease in $\delta(w)$ over a small range of w is reasonable, as may be seen from Figure 16. This amounts to approximation of the curve by a series of straight line segments between successive $\delta(w)$ values. The successive w-values have been taken sufficiently close together that this is a good approximation, especially for the higher w-values where the $\delta(w)$ curve has levelled off.

Thus at w = 3.16 the imaginary part of $1/W(jw)$ is taken to be - 0.025, and $\delta(w)$ is 0.024. At w = 3.17, however, the imaginary part is - 0.023, while $\delta(w)$ is still approximately 0.024. Therefore, w_ℓ is estimated to be 3.16 rad./sec. Similarly, w_h is found to be 3.42 rad./sec. The frequency range is therefore

$$3.16 \leq w \leq 3.42 \qquad (B - 6)$$

The describing function amplitude and frequency predictions are found from the intersection of the two loci, which, from equation (B - 1), occurs at $w^2 = 11$, giving a value of 60/130 = 0.461 on the describing function. The predictions are:

$$\left.\begin{aligned} A_b &= 1.77 \\ w_b &= \sqrt{11} = 3.32 \text{ rad./sec.} \end{aligned}\right\} \qquad (B - 7)$$

The bound on $|x_h(t)|$, from equation (III - 3), is

$$\text{Bound on } |x_h(t)| = \frac{\pi A_h}{4M_1}\,\delta(w_\ell)$$

$$= \frac{\pi(2.09)}{4(0.5)} \quad (0.024)$$

$$= 0.079 \qquad (B - 8)$$

Finally, the bound on max $|x(t)|$ is

$$\max|x(t)| \leq A_h + 0.08 = 2.09 + 0.08 = 2.17 \qquad (B - 9)$$

APPENDIX C

ANALOG SIMULATION AND EXPERIMENTAL PROCEDURE

Simulation of Rankine's $G_1(s)$ - plus - saturation system

Using Rankine's representation of the nonlinear system[1] and introducing minus signs in the numerator and denominator of the linear transfer function, one can write

$$\frac{-C(s)}{-Y(s)} = G_1(s) = \frac{K}{(s+1)(s+2)(s+3)} = \frac{K}{s^3+6s^2+11s+6}$$

where K has been used to represent the gain of the linear element, since it will be varied. The differential equation for the linear element will be

$$p^3(-c) + 6p^2(-c) + 11p(-c) + 6(-c) = K(-y)$$

or, with division by ten throughout,

$$p^3\left(\frac{-c}{10}\right) = 6p^2\left(\frac{c}{10}\right) + 11p\left(\frac{c}{10}\right) + 6\left(\frac{c}{10}\right) + K\left(\frac{-y}{10}\right) \qquad (C-1)$$

The saturation nonlinearity was simulated by using two comparators to produce different portions of the characteristic and summing their outputs. Figure 18 shows the desired characteristic, with the "knee" at 1.5 [2] but with provision being made to vary the slope M_1. Figure 19 shows the individual outputs of the two comparators, and Figure 20 shows the sum of the two comparator outputs. The sum of the two comparator outputs could be multiplied by the appropriate value of M_1 to

---

[1] Rankine, op. cit., Figure 1 (b) on page 11.

[2] Ibid. In the diagram on page 29 the "knee" of the saturation nonlinearity occurs at an input of S/2, while on page 36 it is noted that S = 3 was chosen.

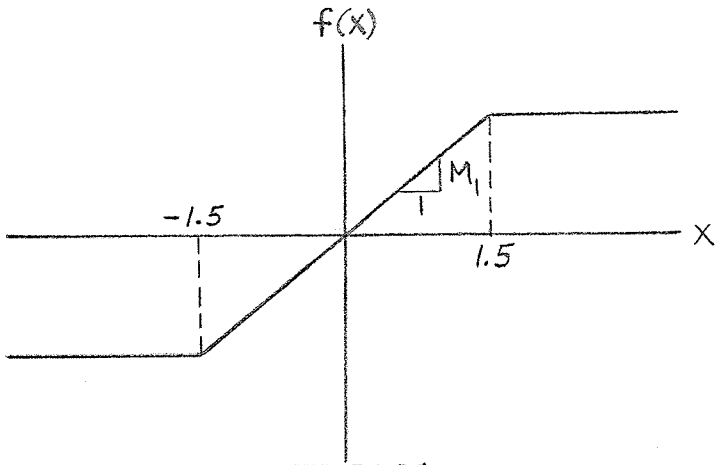

FIGURE 18

DESIRED SATURATION CHARACTERISTIC

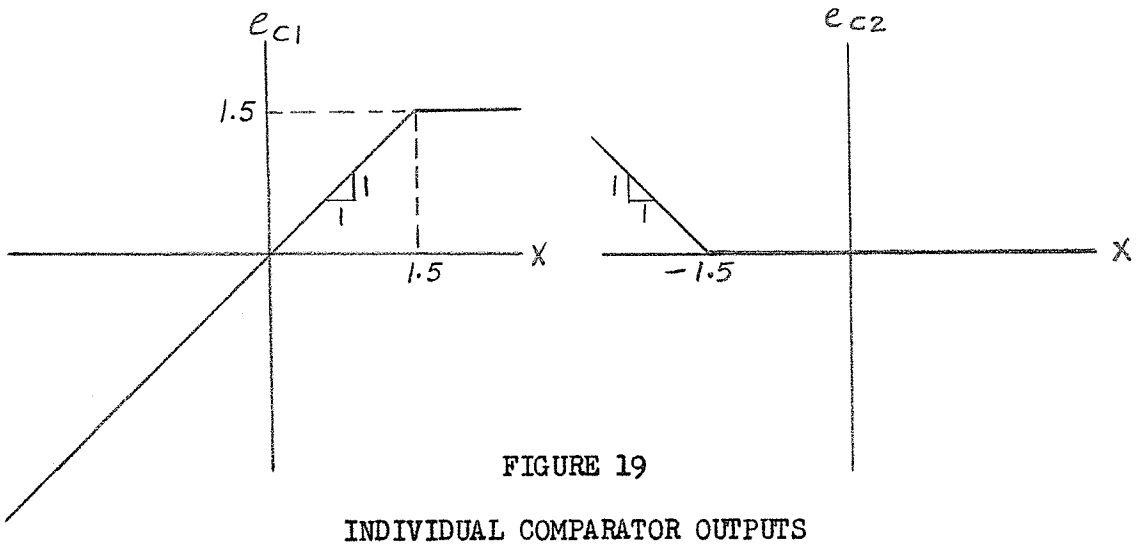

FIGURE 19

INDIVIDUAL COMPARATOR OUTPUTS

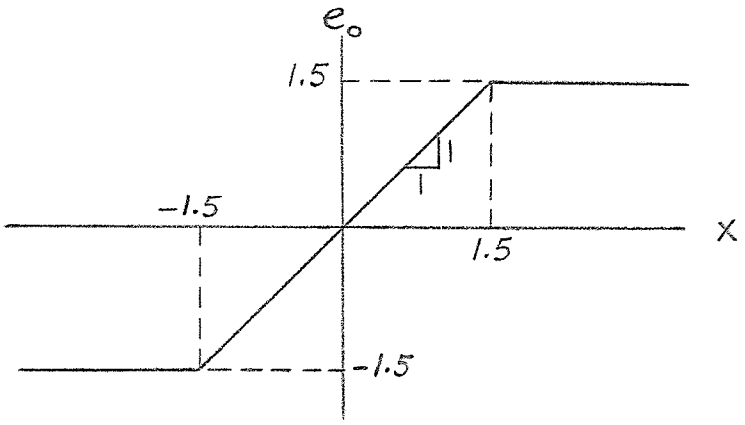

FIGURE 20

SUM OF COMPARATOR OUTPUTS

give the desired nonlinear characteristic for an individual trial. Checks of the different characteristics by sweeping the input from -10 volts to +10 volts revealed that this method provided an excellent simulation of the saturation nonlinearity.

Figure 21 is the simulation diagram for the entire system. In each trial potentiometer 15 was set at K/1000, K being the desired gain of the linear element, and potentiometer 20 was set at M_1, the desired slope of the nonlinear characteristic. An initial condition could be applied to x, the input to the nonlinear element, through integrator 30, and x was available for plotting at the output of amplifier 29.

Amplitude measuring circuit

Figure 22 shows the analog computer circuit used for measuring limit cycle amplitudes. It involves a comparator and an integrator. The inputs to the comparator were x, the oscillation whose amplitude was to be measured, and the signal fed back from the output of the integrator. The comparator was set to give an output of 10 volts or 0 volts, depending on the polarity of the sum of the two inputs. If the comparator output were 0 volts, the output of the integrator would, of course, hold at the value it had reached. If, on the other hand, the comparator output were 10 volts, the output of the integrator would be a negative-going ramp.

The comparator was set up to give the 10 volt output when the sum of the inputs was positive. This meant that if x started at a positive initial condition the integrator would begin to give a negative

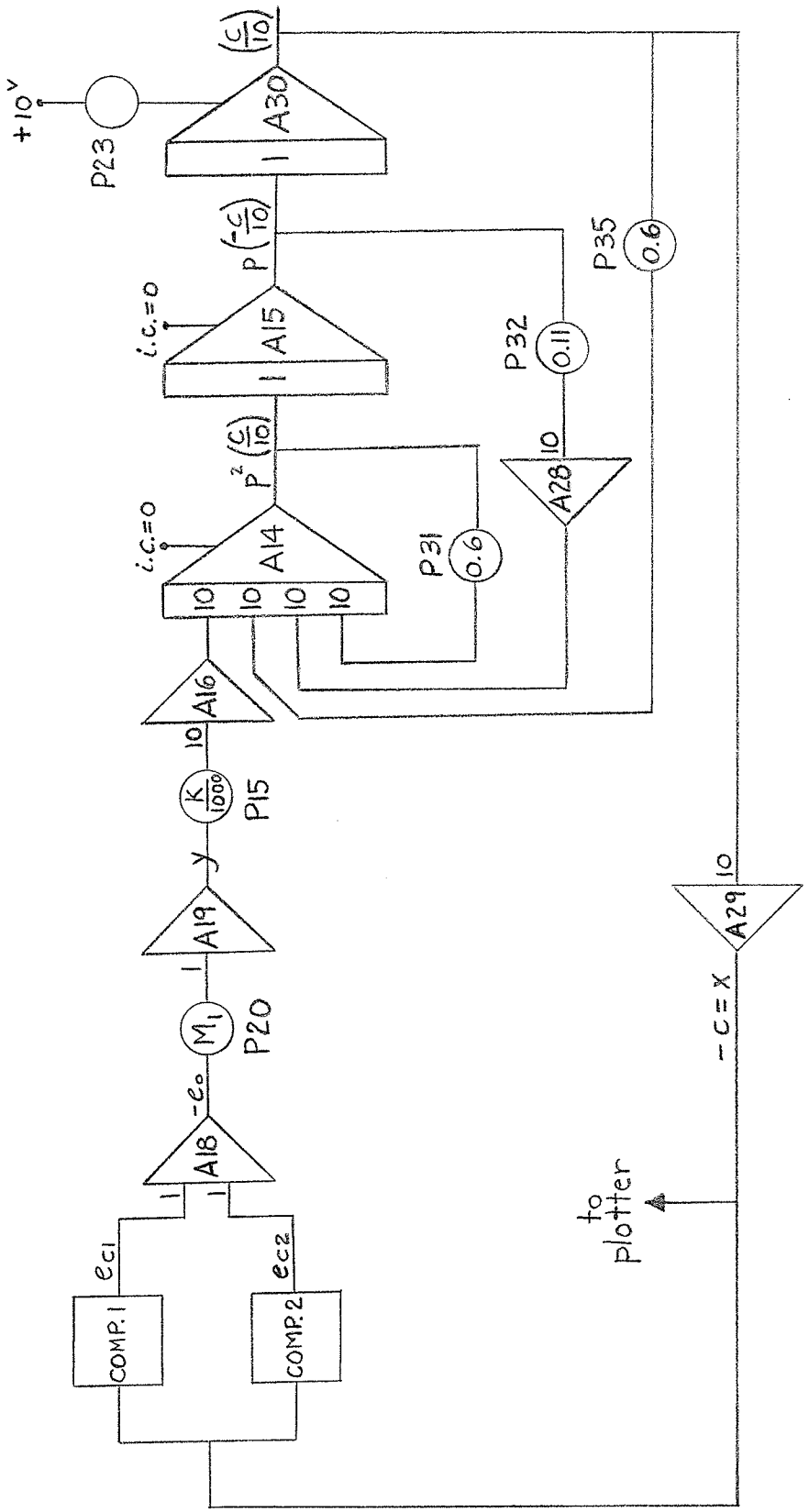

FIGURE 21

SIMULATION DIAGRAM FOR RANKINE'S $G_1(s)$ - PLUS - SATURATION SYSTEM

ramp. The integrator output would hold its value when the sum of the inputs became negative, then would continue the negative ramp when the sum of the inputs became positive again. Thus the integrator output would build up until it eventually reached the negative of the amplitude of x, at which point it would stop. In all the trials the integrator output reached its final value after about five cycles of the x(t) waveform.

This method for limit cycle amplitude measurement was chosen because it eliminated the plotter entirely. The amplitude could be read directly on the computer's digital voltmeter at the output of integrator 11. The maximum error that an amplitude reading could possibly have was -0.01, since the digital voltmeter truncated the third decimal place. This, it was felt, was better than the accuracy that could be obtained with a measurement technique involving the plotter.

Two precautions were necessary when this amplitude measuring circuit was used. First, to initiate a limit cycle an initial condition lower than the expected amplitude of oscillation had to be used so that the oscillation would build up to its final amplitude. Otherwise the integrator output could possibly hold at a higher value than the true amplitude. Second, it was necessary to ensure that when the 0 volt reference of the comparator was selected the comparator output was exactly 0 volts. Otherwise the integrator output would never hold a steady value. It was found that the comparator gave a positive output of between 1 and 2 millivolts when the 0 volt reference was selected. Therefore, this reference was made slightly positive, so that the comparator

output read 0.00 volts after two stages of multiplication by 10. With this modification the output of integrator 11 behaved exactly as planned. As the various trials were run, several checks were made to ensure that the 0 volt comparator output was maintained.

Simulation of second Garber - Rozenvasser example system

The differential equation for the autonomous example system is

$$(p^2 + 0.8p + 8)x = p\, f(x) = p\, y$$

Hence

$$p^2(x) + 0.8p(x) + 8(x) = p(y)$$

or

$$p(x) = -0.8(x) - 8\left(\frac{x}{p}\right) + y \qquad (C - 2)$$

The saturation nonlinearity was simulated with two comparators as before, the "knee" coming this time at 1.0 and the slope being fixed at 1:1. Figure 23 is the simulation diagram for the entire system. A positive initial condition could be applied to the response x through integrator 14, and x was available for plotting at the output of amplifier 29.

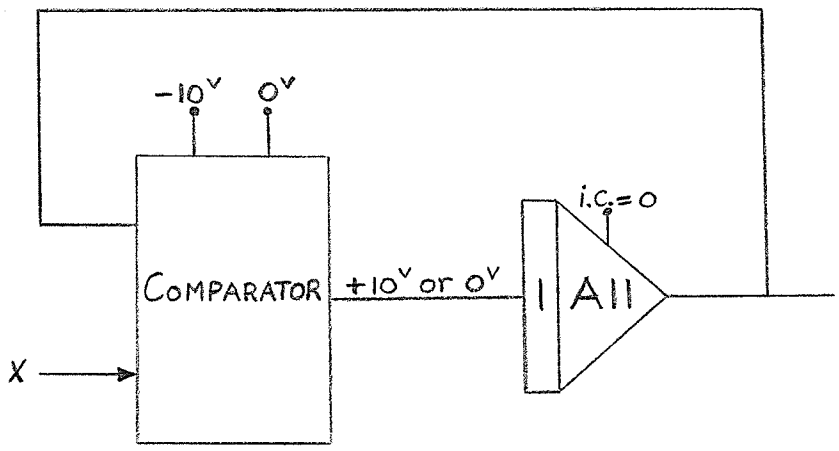

FIGURE 22

AMPLITUDE MEASURING CIRCUIT

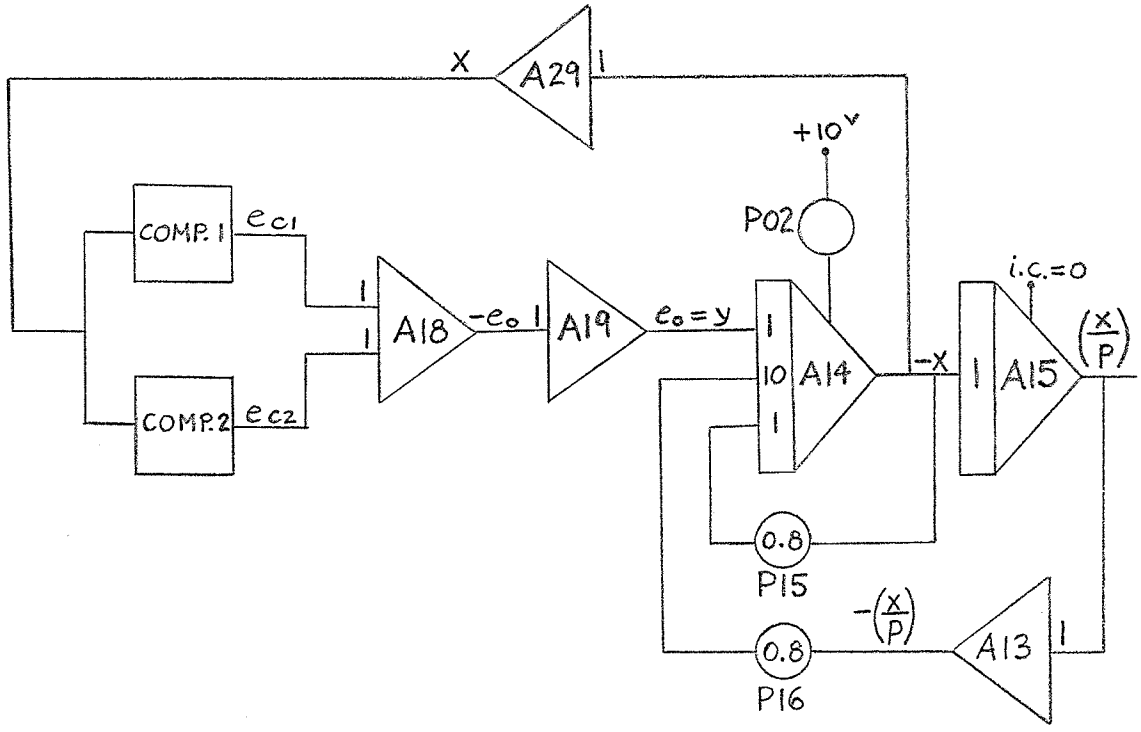

FIGURE 23

SIMULATION DIAGRAM FOR SECOND GARBER-ROZENVASSER EXAMPLE SYSTEM